Induction of APOBEC3B expression by chemotherapy drugs is mediated by DNA-PK directed activation of NF-κB

Manikandan Periyasamy[1], Anup K Singh[1], Carolina Gemma[1], Raed Farzan[1, 6], Rebecca C Allsopp[2], Jacqueline A Shaw[2], Sara Charmsaz[3], Leonie S Young[3], Paula Cunnea[1], R Charles Coombes[1], Balázs Győrffy[4, 5], Lakjaya Buluwela[1], Simak Ali[1, *]

[1]Department of Surgery & Cancer, Imperial College London, London W12 0NN, UK

[2]Department of Cancer Studies and Cancer Research UK Leicester Centre, University of Leicester, Leicester, UK

[3]Endocrine Oncology Research Group, Department of Surgery, Royal College of Surgeons in Ireland, Dublin, Ireland.

[4]Semmelweis University Department of Bioinformatics and 2nd Department of Pediatrics, Budapest, Hungary

[5]MTA TTK Lendület Cancer Biomarker Research Group, Institute of Enzymology, Budapest, Hungary

[6]Present address: Department of Clinical Laboratory Sciences, College of Applied Medical Sciences, King Saud University, Riyadh, Saudi Arabia

Running title: ATM/DNA-PKcs activated NF-κB drives APOBEC3B expression

Keywords: Cancer, cancer mutations, cytosine deaminases, APOBEC3, chemotherapy, NF-κB

* Author for correspondence: Simak Ali, Department of Surgery & Cancer, Imperial College London, Du Cane Road, London W12 0NN, UK; Email: simak.ali@imperial.ac.uk

The authors declare no conflict of interest

Abstract

The mutagenic APOBEC3B (A3B) cytosine deaminase is frequently over-expressed in cancer and promotes tumour heterogeneity and therapy resistance. Hence, understanding the mechanisms that underlie A3B over-expression is important, especially for developing therapeutic approaches to reducing A3B levels, and consequently limiting cancer mutagenesis. We previously demonstrated that A3B is repressed by p53 and p53 mutation increases A3B expression. Here, we investigate A3B expression upon treatment with chemotherapeutic drugs that activate p53, including 5-fluorouracil, etoposide and cisplatin. Contrary to expectation, these drugs induced A3B expression and concomitant cellular cytosine deaminase activity. A3B induction was p53-independent, as chemotherapy drugs stimulated A3B expression in p53 mutant cells. These drugs commonly activate ATM, ATR and DNA-PKcs. Using specific inhibitors and gene knockdowns, we show that activation of DNA-PKcs and ATM by chemotherapeutic drugs promotes NF-kB activity, with consequent recruitment of NF-kB to the A3B gene promoter to drive A3B expression. Further, we find that A3B knockdown re-sensitises resistant cells to cisplatin, and A3B knockout enhances sensitivity to chemotherapy drugs. Our data highlight a role for A3B in resistance to chemotherapy and indicate that stimulation of A3B expression by activation of DNA repair and NF-kB pathways could promote cancer mutations and expedite chemoresistance.

Introduction

Apolipoprotein B mRNA editing catalytic polypeptides (APOBECs) form a family of zinc-dependent cytidine deaminases that, in humans, include activation-induced deaminase (AID), APOBEC1, APOBEC2, APOBEC4 and seven APOBEC3 genes (A3A, A3B, A3C, A3D, A3F, A3G and A3H) [1]. Members of the APOBEC3 subfamily are capable of deaminating cytidine-to-uridine (C-to-U) on single stranded DNA (ssDNA), to generate potential cytidine-to-thymine (C-to-T) transition and cytidine-to-guanine (C-to-G) transversion mutations in 5'-TC motifs [2]. As part of the innate immune system, APOBEC3 genes are implicated in defence against viral pathogens such as retroviruses, papillomaviruses, hepatitis virus, and in the restriction of endogenous retroelements. Numerous studies have revealed the capacity of APOBEC3 proteins to cause genomic DNA mutation [3-5]. Concomitant with these reports has been the understanding, in the wake of cancer genome sequencing, that APOBEC3 cytidine deaminase activity drives somatic mutations in many cancers, including breast, ovarian, head and neck, and lung cancer [5-7]. The most compelling evidence links A3B to these cancer mutations, [2, 5, 7, 8], with A3B-mediated mutagenesis implicated in localised clustering of mutations (kataegis) [4], generation of cancer driver mutations in PIK3CA and TP53 [8-10] and triggering of tumour heterogeneity [9], which may drive tumour evolution [11] and resistance to cancer therapies [12, 13].

The induction of APOBEC3 expression following the interferon response upon viral infection is well-established [14]. Less clear are the mechanisms by which APOBEC3 overexpression, and particularly A3B, are elevated in cancer. We previously showed that p53 is an important repressor of A3B expression in diverse cancer types [15]. Surprisingly, chemotherapy agents stimulated, rather than inhibited, A3B expression, despite their activation of p53. Indeed, induction of A3B expression by these drugs was p53-independent. Using chemical inhibitors, siRNA and CRISPR-Cas9 knockout cells, together with expression analysis and chromatin immunoprecipitations (ChIP), we now show that chemotherapy induction of A3B expression and activity, as well as A3B-directed activation of base excision repair (BER) is directed by DNA-PKcs/ATM/AKT activation of NF-κB. We provide evidence for elevated levels of activated ATM, DNA-PKcs, NF-κB and associated higher A3B expression in ovarian cancer cell lines derived from patients following progression on cisplatin, suggesting that activation

of this pathway may underlie continued mutational activity in the generation of chemotherapy resistance and tumour evolution. Importantly, through CRISPR mediated gene knockout, and siRNA studies, we also show that sensitivity to chemotherapy agents is modulated by A3B.

Results

Chemotherapeutic drugs stimulate A3B expression in cancer cells

To determine if A3B expression was correlated with response to chemotherapy treatments, we analysed two large, independent, breast cancer patient public gene expression data sets. Chemotherapy-treated breast cancer patients with higher A3B expression, progressed more rapidly than those with lower A3B expression in both data sets (Figure 1A-B). High A3B expression has been associated with poor outcome in ER+ breast cancer [16]. Dividing patients in this ER+ cohort into chemotherapy responders and non-responders, showed that non-responder groups were characterised by significantly higher A3B expression than responder groups (Mann-Whitney U test in the GEO series $p=6.97x10^{-6}$ and in the METABRIC p=0.00036, respectively) (Figure 1C-D). Analysis of ER+ patients who received chemotherapy, but who were not treated with hormonal therapy, further confirms a greater incidence of recurrence with high A3B expression (HR = 1.8 (1.21-2.67), logrank p=0.003) (Supplementary Figure 1).

To better understand response to chemotherapy *in vitro*, we deleted the A3B gene in the ER+ MCF7 breast cancer cell line. Interestingly, A3B knockout increased the sensitivity of MCF7 cells to chemotherapy agents (Figure 1E). Additionally, all treatments stimulated A3B expression in p53-WT MCF7 cells (Figure 1F), a response that was confirmed in the p53-WT HCT116 cells (Figure 2A, 2B). As we reported previously that p53 suppress A3B expression, we anticipated that the chemotherapy agents would also repress A3B expression. Contrary to our expectations, all agents increased A3B expression in a p53-independent manner; A3B expression was stimulated by chemotherapy agents in p53-WT and p53-null HCT116 and other p53-WT and -mutant breast cancer cells (Supplementary Figure 2A-B). Expression of other APOBEC3 genes, namely A3C and A3H, was also induced by chemotherapy drugs, but this increase was strictly p53-dependent, consistent with direct p53 regulation of their expression, as reported previously [17]. ChIP-qPCR showed that Nutlin-3A, an activator of p53 [18], as well as etoposide and cisplatin, promote p53 recruitment to the A3C and A3H gene promoters (Figure 2C). This was confirmed by analysis of published p53 ChIP-seq data (results of one ChIP-seq data set [19] are shown (Figure 2D). However, p53 was not recruited to the A3B promoter (Figure 2C).

A3B expression was also stimulated in a p53-independent manner by hydroxyurea (HU; DNA synthesis inhibitor), SN38 (topoisomerase I inhibitor) and by aphidicolin (DNA polymerase inhibitor), whereas expression of A3C, A3D and A3H by these agents required p53 (Supplementary Figure 2C-D). Stimulation of A3B expression, independent of p53 status, by the chemotherapeutic drugs was also confirmed in MCF7 cells in which p53 has been inactivated using CRISPR-Cas9 genome editing [15] (Supplementary Figure 2D, 2E). Taken together, these results show that a mechanistically broad variety of chemotherapy agents promote A3B expression independent of p53.

Stimulation of A3B expression by chemotherapy agents promotes APOBEC3 activity in cancer cells

The above results demonstrate that chemotherapy drugs stimulate the expression of several APOBEC3 genes, so treatment with these agents should increase cytidine deaminase (CD) activity. To test this, CD activity was assessed with a single-stranded oligonucleotide containing the sequence TCA, which is the optimal substrate for A3B [20] and is an efficient substrate for the other APOBEC3 genes [21, 22]. Consistent with increased levels of A3B and other APOBEC3 genes, CD activity was boosted by etoposide, cisplatin and by 5-FU (Figure 3A-C). However, CD activity was also increased in p53-null cells, implying that the augmentation of CD activity is due to A3B, as expression of other APOBEC3 genes remained low and was unchanged by the drugs in cell lines with mutant p53. Furthermore, CRISPR-Cas9 knockout of A3B expression in MCF7 and HCT116 yielded cells with low CD activity, regardless of drug treatment (Figure 3B-D, Supplementary Figure 2E-F), confirming that CD activity in HCT116 and MCF7 cells is mostly attributable to A3B. We note that expression of other APOBEC3 genes was similar to, or slightly higher in A3B-/- MCF7 cells compared to the parental MCF7 cells and expression increases following Nutlin-3A or chemotherapy treatments were similar to, or a little greater, than those observed in the parental MCF7 cells (Supplementary Figure 2G).

Cytidine deamination by APOBEC3 proteins generates U:G mismatches in genomic DNA, activating the base excision repair (BER) pathway in which uracil DNA glycosylases excise U:G mismatches to generate apurinic/apyrimidinic (AP) sites that are processed by AP

endonuclease and which can be labelled and quantified [23]. All drugs increased global genomic AP sites in p53-WT (CAL51) and in p53 mutant (MDA-MB-453) cells (Figure 3E). Drug treatments similarly increased AP sites in MCF7 cells. AP sites were approximately 2-fold higher in p53-null MCF7 cells and drug treatments further increased AP sites (Figure 3F), consistent with the higher A3B expression in p53-null cells. Since there is low expression of the other APOBEC3 genes following drug treatments in p53-null cells, the increase in AP sites is likely to be due to A3B, as well as BER activation by direct DNA damage by these agents. While a key mechanism of action of 5-FU is through inhibition of thymidylate synthase, 5-FU and its metabolites can be incorporated into DNA, thus activating BER [24]. Intrastrand crosslinks (ICLs) induced by cisplatin and DNA damage induced by topoisomerase inhibitors, such as etoposide, also activate BER, as well as other repair pathways [25, 26]. A3B deletion impaired the stimulation of AP site generation by 5-FU in MCF7 cells by 46% (± SD = 3.9%, p=0.0036) (Figure 3F), further evidence that stimulation of A3B expression represents a mechanism for 5-FU-mediated DNA damage. The number of genomic AP sites were similarly lower in A3B-null MCF7 cells treated with etoposide (mean = 38%, SD = 1.08%, p=0.0004), cisplatin (mean = 28%, SD = 0.66, p=0.0003), hydroxyurea (mean = 48%, SD = 2.8, p=0.0018) and SN38 (mean = 38%, SD = 3.04, p=0.0033). Genomic AP sites were also reduced in A3B-null HCT116 cells by between 19% (SD = 0.77, p=0.0008) in the case of HU and 33% (SD = 3.6, p=0.0061) for cisplatin (Figure 3G). Since there is no reduction in expression of the other APOBEC3 genes in A3B-null cells, these results support the idea that A3B activity is an important driver for BER activation following treatment with diverse DNA damaging chemotherapeutic drugs.

The DREAM complex is not involved in stimulation of A3B expression by chemotherapy

Our previous work showed that repression of A3B expression by p53 involves a pathway in which p53 activation induces p21 expression, which inhibits CDK2/4/6 and so promotes recruitment of the transcriptional repressive E2F4/p107/p130-containing DREAM complex and concomitant displacement of the B-MYB transcriptional activation complex at the A3B gene [15]. As expected, and like Nutlin-3A, both etoposide and cisplatin stimulated p53 recruitment to the p21 and MDM2 gene promoters in ChIP assays (Supplementary Figure 3A), consistent with the activation of p53 by these drugs. By contrast, Nutlin-3A did not support p53 recruitment to the A3B gene, nor was p53 recruited to the survivin gene

(Supplementary Figure 3A), another p53-regulated gene that is repressed by the DREAM complex (see ref [15]). Nutlin-3A stimulated DREAM complex recruitment to the A3B gene, as shown with ChIP for the DREAM complex subunits E2F4 and p130, as well as the E2F4-associated KDM5a/JARID1a H3K4 demethylase [27] (Figure 4A, Supplementary Figure 3A). This was accompanied by reduced B-MYB, p300, CBP and RNA polymerase II (PolII) at the A3B gene promoter. By contrast, DREAM complex recruitment was not stimulated by etoposide or cisplatin. Moreover, these treatments resulted in increased binding of the histone acetyltransferases CBP and p300, H3K27 acetylation (H3K27ac) and PolII recruitment, indicative of DREAM complex-independent induction of A3B expression by these drugs. Moreover, and consonant with A3B expression, the DREAM complex was not recruited to the A3B promoter in p53-null HCT116 cells, while CBP, p300, PolII and H3K27ac were enriched by etoposide and cisplatin (but not by Nutlin-3A) in p53-null HCT116 cells. In summary, despite the lack of DREAM complex recruitment, chemotherapy treatments did not stimulate B-MYB binding at the A3B promoter, indicating that B-MYB does not mediate the chemotherapy induction of A3B expression.

Chemotherapy drugs promote NF-κB recruitment to the A3B gene promoter to stimulate its expression

Stimulation of A3B expression, through PKC-directed recruitment of the NF-κB RelB subunit, but not of RelA/p65, has recently been reported [28]. However, evidence for regulation of A3B expression by RelA/p65 has also been forthcoming [29]. In agreement with the latter, analysis of reported ChIP-seq data (GSE24518, GSE102796, GSE67295) showed that NF-κB activation induces RelA/p65 recruitment to the A3B gene promoter (Supplementary Figure 3B), with additional binding to a region approximately 10 kb 5' to the A3A gene and a region upstream of the A3G gene. Consistent with this, RelA/p65, p50, RelB and p52 were recruited to the A3B gene upon addition of etoposide and cisplatin in HCT116, p53-null HCT116 and in p53-mutant T47D cells (Figure 4B-C); the results were suggestive of greater recruitment of RelA/p65 and p50 than of RelB or p52. Etoposide and cisplatin similarly promoted NF-κB recruitment to well-characterised NF-κB target genes (ICAM1, IL8, CXCL1), generally with greater enrichment of p65 and p50 than of RelB and p52 (Supplementary Figure 3C-D). NF-κB recruitment following etoposide or cisplatin treatment occurred irrespective of p53

status and NF-κB recruitment was not influenced by Nutlin-3A. The NF-κB inhibitors, BAY 11-7082 [30] and TPCA-1 [31] reduced NF-κB recruitment to the A3B gene promoter (Figure 4D, Supplementary Figure 4A) and blocked stimulation of A3B expression by cisplatin, etoposide or HU (Figure 4E-F, Supplementary Figure 4B-C). Consistent with NF-κB recruitment primarily at the A3B promoter (Supplementary Figure 3B), NF-κB inhibitors largely did not affect the chemotherapy-stimulated expression of other APOBEC3 genes (Supplementary Figure 4C). Finally, siRNA-mediated p65/p50 knockdown also blunted the stimulation of A3B expression by cisplatin and etoposide (Supplementary Figure 4D). Thus, DNA damage by cytotoxic drugs activates NF-κB, which, in turn, drives A3B expression.

DNA-PKcs and ATM mediate NF-κB-directed expression of the APOBEC3B gene

The DNA damage response activated upon genotoxic stress is mediated by three related kinases, ATM, ATR and DNA-PKcs, with ATM and DNA-PKcs being central to the response to DNA double strand breaks (DSB) formation of the type engendered by cytotoxic chemotherapies [32]. Moreover, ATM activates NF-κB through a mechanism in which interaction of ATM with the the regulatory subunit of IκB kinase (IKKγ, also known as the NF-κB essential modulator, NEMO), promotes its export to the cytoplasm, facilitating IκB phosphorylation and consequent degradation [33] (Figure 5A). DNA-PKcs can also activate NF-κB, by directly phosphorylating IκB [34] and via activation of AKT [35], a key mediator of IκB kinase [36]. Therefore, we determined if the chemotherapy induced expression of A3B results from activation of NF-κB signaling by these DNA damage response (DDR) kinases [37].

In T47D cells, the DNA-PKcs inhibitor, NU7441, inhibited A3B expression in a dose-dependent manner, whereas ATM (KU55933) and ATR (VE-821) inhibitors had only small effects on A3B mRNA levels (Figure 5B, Supplementary Figure 5A). Similar results were obtained in HCT116 cells, except that the highest dose of VE-821 inhibited expression of all A3 genes (Supplementary Figure 5B). Although VE-821 reduced basal A3B expression, it only modestly suppressed the cisplatin and etoposide induction of A3B expression, by 22% (SEM ± 5.01, p=0.0001) and 28% (SEM ± 1.04, p=0.0001), respectively (Supplementary Figure 5C). This compares with 55% (SEM ± 1.1, p=0.0001) and 50% (SEM ± 1.3, p=0.0001) inhibition of

the cisplatin and etoposide mediated increase in A3B expression by KU55933 (Supplementary Figure 5C). NU7441 reduced the cisplatin and etoposide induction of A3B by 68% (SEM ± 0.7, p=0.0001) and 66% (SEM ± 1.9, p=0.0001) (Figure 5C).

Knockdown of each DDR kinase confirmed the importance of DNA-PKcs and ATM in directing chemotherapy-induced A3B expression. Whereas ATR knockdown had no effect on A3B expression (Supplementary Figure 5D), DNA-PK and ATM siRNA significantly reduced the impact of cisplatin and etoposide on A3B expression. Immunoblotting showed that DNA-PKcs and ATM inhibitors lessened A3B induction by cisplatin/etoposide (Figure 5D, Supplementary Figure 5E), confirming the RT-qPCR results. These findings demonstrate the importance of ATM and DNA-PKcs activities for inducing A3B expression by chemotherapy drugs.

DNA-PKcs activation of NF-κB in promoting A3B expression is mediated via ATM and AKT

NU7441 inhibited the action of cisplatin/etoposide in all cell lines, regardless of p53 status (Supplementary Figure 6A-F). Previous reports show that lack of DNA-PKcs causes ATM down-regulation [38], providing an explanation for the reduction in ATM mRNA and protein levels observed for NU7441 addition or following DNA-PKcs knockdown (Supplementary Figure 5D, Supplementary Figure 7A-B). Chemical inhibition or knockdown of DNA-PKcs also reduced AKT phosphorylation at the activating serine-473 (S473) (Supplementary Figure 7A, B), in agreement with previous reports [36]. Taken together, these results demonstrate the key role of DNA-PKcs in regulating the induction of A3B expression by DNA damaging drugs.

When activated, IκB kinase (IKKα/ß/γ) phosphorylates IκB, which promotes its ubiquitination and subsequent proteasomal degradation, allowing nuclear translocation of NF-κB and consequent activation of NF-κB target genes [36] (Figure 5A). Cisplatin/etoposide increased IKKα/ß and IκBα phosphorylation (Fig 4F), which was prevented by chemical inhibition or siRNA-knockdown of DNA-PKcs (Figure 5D, 5E). Consequently, NU7441 inhibited NF-κB recruitment to the A3B gene promoter tiggered by cisplatin, etoposide and hydroxyurea (Supplementary Figure 8).

KU55933 also reduced A3B levels and strongly inhibited IKKα/β, IκBα phosphorylation, but had only a small effect on DNA-PKcs phosphorylation (Supplementary Figure 5E). Finally, the AKT inhibitor MK2206, inhibited phosphorylation of IKKα/ß, without affecting ATM or DNA-PKcs phosphorylation induced by cisplatin or etoposide (Supplementary Figure 7C). Taken together, these results reveal that NF-κB induces A3B expression in response to DNA damaging drugs and that its activation is mediated by ATM, AKT and DNA-PKcs, with DNA-PKcs having a pivotal role in regulating the chemotherapy-induced activation of NF-κB, via ATM and AKT. Stimulation of A3B expression by this mechanism is consistent with the cytidine deaminase activity in cancer cells, since inhibiting DNA-PKcs, ATM, AKT or NF-κB robustly reduced cisplatin and etoposide stimulation of cytidine deamination activity in lysates from T47D cells (Figure 5F,G).

Finally, we determined if this pathway also stimulated A3B expression in the non-tumourigenic breast epithelial MCF10A cell line. As in all cancer cell lines tested, chemotherapy drugs stimulated A3B expression (Supplementary Figure 9A). A3B expression was also induced in primary metastatic breast cancer cells (PEOO3), obtained from a pleural effusion [39] (Supplementary Figure 9B). In MCF10A, as well as PEOO3 and in primary normal human mammary epithelial cells (HMEC), DNA-PK, ATM, AKT or NF-κB inhibitors reduced cisplatin-induced A3B expression and cellular cytidine deaminase activity. Together, these results demonstrate that this mechanism for A3B induction is not restricted to established cancer cell lines.

The DNA-PKcs/AKT/ATM/NF-κB axis is constitutively active and A3B expression is upregulated in platinum-resistant high-grade serous ovarian carcinoma cells

High-grade serous ovarian carcinoma (HGSOC) shows a high degree of genomic instability, copy number alterations, p53 mutation and chemoresistance. Platinum based chemotherapy is used as first-line therapy for the treatment of HGSOC [40], but most patients progress with platinum-resistant disease. Increased DNA-PKcs activity and DNA-PKcs-directed activation of AKT has also been proposed as a mechanism for driving resistance to platinum in ovarian cancer cells [41]. Therefore, we wondered if the increased DNA-PKcs and AKT activity in platinum-resistant cancer cells, is accompanied by NF-κB

activation and higher A3B expression. To this end, we used the isogenic HGSOC paired cell lines PEA1, an HGSOC cell line generated from a patient prior to cisplatin treatment and PEA2, obtained from the same patient following relapse after cisplatin treatment [42].

A3B expression was considerably higher in the cisplatin-resistant PEA2 cells, compared with PEA1 cells (Figure 6A-B). Expression of other NF-κB target genes was also elevated in PEA2 cells than in PEA1 cells, indicative of higher NF-κB activity in the cisplatin-resistant cells. Immunoblotting confirmed higher activities of DNA-PKcs, AKT, ATM and NF-κB, as defined by the phosphorylation levels of DNA-PKcs, ATM, AKT, IKK and IκB in PEA2 cells (Figure 6B). Together with higher A3B expression and cytidine deaminase activity in PEA2 over PEA1 cells (Figure 6C) and the greater enrichment of p65/p50 NF-κB subunits at the A3B gene promoter (Figure 6D), these results are consistent with the data linking ATM/NF-κB and DNA-PKcs/AKT/NF-κB in regulating A3B expression and cytidine deaminase activity in response to cisplatin. Inhibiting ATM, DNA-PKcs, AKT or NF-κB reduced expression of A3B in the absence of chemotherapy drugs in the cisplatin-resistant PEA2 cells (Figure 6E), which implies that these pathways are constitutively active in the cisplatin-resistant HGSOC cells and are responsible for A3B expression. Inhibiting NF-κB increased the sensitivity of PEA2 cells to cisplatin, whereas cisplatin-sensitive PEA1 cells were not much affected by TPCA1, consistent with the elevated NF-κB activity PEA2 (Supplementary Figure 10). In keeping with the increased DNA-PK, ATM and AKT activities in PEA2, compared with PEA1 cells, these inhibitors were also more effective in promoting cisplatin-directed growth inhibition in PEA2 cells.

We also determined if the increased expression of A3B in the cisplatin-resistant ovarian cancer cells is associated with the resistance to cisplatin. Interestingly, A3B knockdown re-sensitised the cisplatin-resistant PEA2 cells to cisplatin (Figure 6F), reducing the IC_{50} from 20.5 μM to 6.8 μM (difference between means ± SEM = 13.7 ± 1.0, $p<0.0001$); similar to the IC_{50} values for cisplatin in the cisplatin-sensitive PEA1 cells (5.3 μM) (the difference between means of ± SEM for siA3B-PEA2 and siControl-PEA1 = 1.5 ± 0.5, $p=0.02$). Moreover, A3B knockdown increased cisplatin-induced apoptosis, as judged by the increase in caspase activity, as well as levels of cleaved PARP and γH2AX (Figure 6G, H). A3B knockdown also

increased sensitivity of PEA1 cells to cisplatin, albeit, the reduction in IC_{50} values was much more modest (difference between means ± SEM = 0.4 ± 1.0, p=0.003) (Figure 6F).

Discussion

We have shown that DNA damaging chemotherapy drugs stimulate A3B expression, in a p53-independent manner, suggesting that these agents promote A3B expression by a mechanism that is distinct from the DREAM transcription repression complex, previously reported as the mediator of p53-directed A3B inhibition [15]. Compatible with this proposition, treatment with etoposide or cisplatin did not, promote DREAM complex recruitment to the A3B gene promoter. Unlike the p53 activator, Nutlin-3A, these agents also stimulated recruitment of RNA PolII and CBP/p300 histone acetyltransferases, together with increased H3K27 acetylation at the A3B gene promoter. The action of these drugs acting independently of p53 was confirmed in cell lines expressing mutant p53, or cells in which p53 had been ablated by gene knockout.

As has been shown previously for the DNA damaging agent doxorubicin [17], expression of A3C, A3F, A3D and A3H was stimulated by etoposide, cisplatin and hydroxyurea, but as we also show, stimulation of their expression is dependent on the presence of functional p53. ChIP-qPCR confirmed direct recruitment of p53 to their gene promoters upon addition of Nutlin-3A, or chemotherapy drugs. Although interrogation of public p53 ChIP-seq data did not identify p53 binding sites at the A3D and A3F gene promoters, p53 binding to the upstream A3C gene may be sufficient to provide p53 regulation of A3D and A3F expression. Importantly, the results presented here collectively reveal that the increased cellular cytidine deaminase activity caused by the chemotherapeutic agents is due to A3B, with little or no involvement of the other APOBEC3 genes.

Our results using specific inhibitors of each kinase and siRNA-mediated knockdown, show that DNA-PKcs and ATM are necessary for A3B expression in response to etoposide and cisplatin. ATR, by contrast, did not greatly impact on the etoposide/cisplatin stimulation of A3B expression, despite the fact that ATR is activated by genotoxic stresses [32]. In addition, RNAi and inhibitor data demonstrate clearly the importance of DNA-PKcs and ATM for chemotherapy drug induced expression of A3B.

A3B expression was recently shown to be stimulated by PMA-directed activation of NF-κB [28, 29]. Analysis of published ChIP-seq data showed that RelA (p65) is recruited to the A3B gene promoter following TNFα and/or IL1ß treatments. Our results show that cisplatin and etoposide also promote recruitment of RelA/p50, and to a lesser extent RelB/p52, to the A3B gene promoter and highlight the particular importance of the canonical NF-κB subunits RelA/p50 in mediating the chemotherapy induction of A3B expression. Our results demonstrate that induction of DNA-PKcs and ATM caused by DNA damaging chemotherapy drugs activates NF-κB, which in turn stimulates expression of A3B and promotes A3B-directed cytidine deamination. These findings emphasize the particular importance of DNA-PKcs in regulating A3B expression by relaying signals from chemotherapy-induced DNA damage to ATM and AKT, for activation of NF-κB and are consistent with previous reports of NF-κB activation upon DNA-PKcs activation following DNA damage by genotoxic agents, including ionising radiation (IR), etoposide and doxorubicin [43-47].

To further understand the role of A3B in chemotherapy sensitivity, we developed MCF7 cells, in which the A3B gene was deleted by CRISPR-Cas9 gene editing and have found that these knockout cells displayed greater sensitivity to genotoxic drugs. RNAi-directed A3B knockdown similarly increased sensitivity of ovarian cancer cells to cisplatin and re-sensitised cisplatin-resistant ovarian cancer cells. Genomic mutations caused by A3B are proposed as a mechanism for promoting tumour evolution and facilitating mutations in genes that cause resistance to cancer therapies [6, 12, 48, 49]. However, our results imply that A3B itself, also plays an important role in protecting cancer cells from the growth inhibitory effects of genotoxic drugs. Several potential mechanisms can be envisaged. Firstly, up-regulation of A3B expression by genotoxic drugs may activate BER pathways, to stimulate DNA damage repair and thus reduce the effectiveness of chemotherapeutic drugs. A3B also plays an intriguing role as a transcriptional co-activator for estrogen receptor-α, to promote growth of breast cancer cells [16]. Another role for A3B in gene regulation is highlighted by the observed interaction of A3B with several miRNA precursors [50]. The importance of these transcriptional functions of A3B in the cellular response to genotoxic drugs needs further exploration.

In conclusion, we present evidence that A3B expression is induced by chemotherapy in a p53-independent manner, via DNA-PKcs and ATM mediated activation of the NF-κB pathway, resulting in elevated A3B expression, with possible consequences for the generation of somatic mutations that drive tumour evolution. Offsetting this, our results also highlight a converse role for A3B in protecting cells from genotoxic stress, perhaps through activation of DNA repair pathways. A potential chemoprotective role of A3B may also underlie the increased incidence of breast cancer in women with a germline copy number polymorphism that results in deletion of the A3B gene [51] and the higher APOBEC mutational signature that has been described for patients with the A3B deletion polymorphism, compared with patients lacking the A3B deletion [51]. While a role for A3B in protecting the genome from DNA damage may seem to be at odds with repression of its expression by p53, it has previously been demonstrated that p53 reduces BER, by inhibiting expression of the AP endonuclease, APE1 [52], which processes the apurinic sites that would be generated by DNA glycosylase action on A3B-mediated cytidine deamination. While our study demonstrates an important role for A3B in reducing sensitivity to chemotherapy drugs, segregation of tumours on the basis of A3B levels did not show an association with patient relapse in ER-negative breast cancer [16]. In addition, a trend towards better progression-free survival has been previously noted for clear cell ovarian cancer patients with high A3B expression [53]. In both cases, other factors such as altered DNA repair capacities, for example due to BRCA1/2 mutations and the additional involvement of expression of APOBEC3 proteins in tumour infiltrating cells [54], are all likely to contribute to, and further complicate responses to chemotherapy mediated by DNA damage. Notwithstanding, inhibition of NF-κB activation, with ATM, DNA-PKcs, AKT or with NF-κB inhibitors, does identify a means of limiting chemoresistance and tumour evolution by A3B.

Materials and Methods

Cell lines and culturing

Cell lines, as well as HMEC cells were obtained from ATCC (LGC Standards, UK) and cultured in DMEM containing 10% FCS, except for HMEC cells which were cultured according to supplier instructions. MCF7 p53-/- cells [15] and HCT116 p53-/- cells [55] have been described. The paired high grade serous ovarian carcinoma lines PEA1 and PEA2 [42] were cultured in RPMI containing 10% FCS. PE003 breast cancer cells have been described [39]. All cell lines were routinely monitored for mycoplasma negativity and were regularly genotyped. Details of drugs used in this study are provided in Supplementary table 1.

CRISPR-Cas9 mediated A3B knockout

Details of the scheme for generating the A3B knockout and guide RNA sequences are provided in supplemental information. pCAG-Cas9-GFP [56] was a gift from Kiran Musunuru (Addgene, http://n2t.net/addgene:44719).

siRNA transfections

Cells were transfected by reverse transfection using Lipofectamine RNAiMAX (Invitrogen, Thermofisher Scientific, UK), as described [16].

Proliferation and clonogenic assays

Cell growth was assessed using the sulphorhodamine B assay (SRB), as described previously [16]. For clonogenic assays, 200 cells/well were seeded in 96 well plates, prior to addition of the indicated drugs or vehicle. Cells were incubated with drugs continuously for 14 days, with changes in media ± drug every 4 days. After 14 days of treatment, cells were processed using the SRB method.

RT-qPCR and ChIP-qPCR

Total RNA extraction and RT-qPCR was undertaken using Taqman Gene Expression Assays (Applied Biosystems, UK) qPCR on an ABI 7900HT machine, as described [16]. Chromatin preparation and immunoprecipitation (ChIP) was performed also as described [16]. ChIP

antibodies, Taqman assays and the primer sequences for qPCR are detailed in Supplementary tables.

Immunoblotting and Cytosine Deaminase assays

Cell lysates were prepared in HEPES lysis buffer (25mM HEPES (pH 7.4), 10% glycerol, 150mM NaCl, 0.5% Triton X-100, 1mM EDTA, 1mM $MgCl_2$ and 1mM $ZnCl_2$), supplemented with protease and phosphatase inhibitors (Roche, UK), sonicated, and lysates were immunoblotted as described [15], using antibodies listed in Supplementary tables. The cytosine deaminase assay has also been described [15].

Caspase 3/7 Assay

Cells were seeded in 96-well clear bottom white plates and treated for 24 hours with cisplatin or vehicle. The Caspase-Glo 3/7 Assay was performed according to manufacturer's instructions (Promega, UK).

Apurinic/apyrimidinic (AP) site determination

Genomic DNA was prepared and assayed using the Oxiselect DNA damage ELISA kit (AP sites) (STA-324), according to manufacturer's protocol (Cell Biolabs Inc. San Diego, CA, USA). Aldehyde reactive probe (ARP) DNA standards provided with the kit, facilitated estimation of the number of genomic AP sites.

Analysis of A3B expression in METABRIC breast cancers and GEO data sets

We utilized two independent patient cohorts to assess the correlation to survival and to chemotherapy response in breast cancer patients. Samples for the GEO dataset were identified by searching the GEO repository (https://www.ncbi.nlm.nih.gov/geo/) for chemotherapy-treated datasets with at least 30 samples (PMID: 31020993). Altogether, we have identified 15 datasets (GSE1456, GSE16391, GSE16446, GSE16716, GSE17907, GSE19615, GSE20271, GSE21653, GSE31519, GSE3494, GSE37946, GSE45255, GSE4611, GSE5327 and GSE69031). A second cohort of samples included chemotherapy-treated tumour samples from the METABRIC dataset [57]. Survival analysis was performed by dividing the patient samples into two cohorts using the expression of A3B and the two

cohorts were compared by Cox proportional hazards regression. Response to therapy was assessed by dividing samples into two cohorts by their response status (responders vs. non-responders) and A3B expression was compared between these two groups by the Mann-Whitney U-test.

Statistical analyses

P-values were calculated using the two-tailed t-test in GraphPad Prism version 8.0, for results of at least three replicates.

Acknowledgements

We thank Dr B Vogelstein for p53-null HCT116 cells. We are grateful to Dr S Langdon for the PEA1 and PEA2 lines. Our thanks also go to Drs S Hong and L Magnani for their kind gift of PEOO3 cells. This study was supported by Cancer Research UK grant C37/A18784. We thank the LMS/NIHR Imperial Biomedical Research Centre Flow Cytometry Facility for support. Additional support was provided by the Imperial Experimental Cancer Medicine Centre, Imperial NIHR Biomedical Research Centre, and the Cancer Research UK Imperial Centre. The views expressed are those of the authors and not necessarily those of the NHS, the NIHR or the Department of Health.

References

1 Salter JD, Bennett RP, Smith HC. The APOBEC Protein Family: United by Structure, Divergent in Function. *Trends in biochemical sciences* 2016; 41: 578-594.

2 Venkatesan S, Rosenthal R, Kanu N, McGranahan N, Bartek J, Quezada SA *et al*. Perspective: APOBEC mutagenesis in drug resistance and immune escape in HIV and cancer evolution. *Annals of oncology : official journal of the European Society for Medical Oncology / ESMO* 2018; 29: 563-572.

3 Nowarski R, Wilner OI, Cheshin O, Shahar OD, Kenig E, Baraz L *et al*. APOBEC3G enhances lymphoma cell radioresistance by promoting cytidine deaminase-dependent DNA repair. *Blood* 2012; 120: 366-375.

4 Taylor BJ, Nik-Zainal S, Wu YL, Stebbings LA, Raine K, Campbell PJ *et al*. DNA deaminases induce break-associated mutation showers with implication of APOBEC3B and 3A in breast cancer kataegis. *Elife* 2013; 2: e00534.

5 Burns MB, Temiz NA, Harris RS. Evidence for APOBEC3B mutagenesis in multiple human cancers. *Nat Genet* 2013; 45: 977-983.

6 McGranahan N, Favero F, de Bruin EC, Birkbak NJ, Szallasi Z, Swanton C. Clonal status of actionable driver events and the timing of mutational processes in cancer evolution. *Science translational medicine* 2015; 7: 283ra254.

7 Roberts SA, Lawrence MS, Klimczak LJ, Grimm SA, Fargo D, Stojanov P *et al*. An APOBEC cytidine deaminase mutagenesis pattern is widespread in human cancers. *Nat Genet* 2013; 45: 970-976.

8 Burns MB, Lackey L, Carpenter MA, Rathore A, Land AM, Leonard B *et al*. APOBEC3B is an enzymatic source of mutation in breast cancer. *Nature* 2013; 494: 366-370.

9 de Bruin EC, McGranahan N, Mitter R, Salm M, Wedge DC, Yates L *et al*. Spatial and temporal diversity in genomic instability processes defines lung cancer evolution. *Science* 2014; 346: 251-256.

10 Poulos RC, Wong YT, Ryan R, Pang H, Wong JWH. Analysis of 7,815 cancer exomes reveals associations between mutational processes and somatic driver mutations. *PLoS Genet* 2018; 14: e1007779.

11 Roper N, Gao S, Maity TK, Banday AR, Zhang X, Venugopalan A *et al*. APOBEC Mutagenesis and Copy-Number Alterations Are Drivers of Proteogenomic Tumor Evolution and Heterogeneity in Metastatic Thoracic Tumors. *Cell Rep* 2019; 26: 2651-2666 e2656.

12 Law EK, Sieuwerts AM, LaPara K, Leonard B, Starrett GJ, Molan AM *et al*. The DNA cytosine deaminase APOBEC3B promotes tamoxifen resistance in ER-positive breast cancer. *Sci Adv* 2016; 2: e1601737.

13 Schmitt C, Lucius R, Synowitz M, Held-Feindt J, Hattermann K. APOBEC3B is expressed in human glioma, and influences cell proliferation and temozolomide resistance. *Oncol Rep* 2018; 40: 2742-2749.

14 Refsland EW, Stenglein MD, Shindo K, Albin JS, Brown WL, Harris RS. Quantitative profiling of the full APOBEC3 mRNA repertoire in lymphocytes and tissues: implications for HIV-1 restriction. *Nucleic Acids Res* 2010; 38: 4274-4284.

15 Periyasamy M, Singh AK, Gemma C, Kranjec C, Farzan R, Leach DA *et al*. p53 controls expression of the DNA deaminase APOBEC3B to limit its potential mutagenic activity in cancer cells. *Nucleic acids research* 2017; 45: 11056-11069.

16 Periyasamy M, Patel H, Lai CF, Nguyen VTM, Nevedomskaya E, Harrod A *et al*. APOBEC3B-Mediated Cytidine Deamination Is Required for Estrogen Receptor Action in Breast Cancer. *Cell Rep* 2015; 13: 108-121.

17 Menendez D, Nguyen TA, Snipe J, Resnick MA. The Cytidine Deaminase APOBEC3 Family Is Subject to Transcriptional Regulation by p53. *Molecular cancer research : MCR* 2017; 15: 735-743.

18 Vassilev LT, Tovar C, Chen S, Knezevic D, Zhao X, Sun H *et al*. Selective small-molecule inhibitor reveals critical mitotic functions of human CDK1. *Proceedings of the National Academy of Sciences of the United States of America* 2006; 103: 10660-10665.

19 Andrysik Z, Galbraith MD, Guarnieri AL, Zaccara S, Sullivan KD, Pandey A *et al*. Identification of a core TP53 transcriptional program with highly distributed tumor suppressive activity. *Genome research* 2017; 27: 1645-1657.

20 Green AM, Weitzman MD. The spectrum of APOBEC3 activity: From anti-viral agents to anti-cancer opportunities. *DNA Repair (Amst)* 2019; 83: 102700.

21 Stenglein MD, Burns MB, Li M, Lengyel J, Harris RS. APOBEC3 proteins mediate the clearance of foreign DNA from human cells. *Nature structural & molecular biology* 2010; 17: 222-229.

22 McDaniel YZ, Wang D, Love RP, Adolph MB, Mohammadzadeh N, Chelico L *et al*. Deamination hotspots among APOBEC3 family members are defined by both target site sequence context and ssDNA secondary structure. *Nucleic acids research* 2020; 48: 1353-1371.

23 Kubo K, Ide H, Wallace SS, Kow YW. A novel, sensitive, and specific assay for abasic sites, the most commonly produced DNA lesion. *Biochemistry* 1992; 31: 3703-3708.

24 Wyatt MD, Wilson DM, 3rd. Participation of DNA repair in the response to 5-fluorouracil. *Cell Mol Life Sci* 2009; 66: 788-799.

25 Wilson DM, 3rd, Seidman MM. A novel link to base excision repair? *Trends Biochem Sci* 2010; 35: 247-252.

26 Pommier Y, Huang SY, Gao R, Das BB, Murai J, Marchand C. Tyrosyl-DNA-phosphodiesterases (TDP1 and TDP2). *DNA Repair (Amst)* 2014; 19: 114-129.

27 Beshiri ML, Holmes KB, Richter WF, Hess S, Islam AB, Yan Q *et al*. Coordinated repression of cell cycle genes by KDM5A and E2F4 during differentiation. *Proceedings of the National Academy of Sciences of the United States of America* 2012; 109: 18499-18504.

28 Leonard B, McCann JL, Starrett GJ, Kosyakovsky L, Luengas EM, Molan AM *et al*. The PKC/NF-kappaB signaling pathway induces APOBEC3B expression in multiple human cancers. *Cancer research* 2015; 75: 4538-4547.

29 Maruyama W, Shirakawa K, Matsui H, Matsumoto T, Yamazaki H, Sarca AD *et al*. Classical NF-kappaB pathway is responsible for APOBEC3B expression in cancer cells. *Biochemical and biophysical research communications* 2016; 478: 1466-1471.

30 Strickson S, Campbell DG, Emmerich CH, Knebel A, Plater L, Ritorto MS *et al*. The anti-inflammatory drug BAY 11-7082 suppresses the MyD88-dependent signalling network by targeting the ubiquitin system. *The Biochemical journal* 2013; 451: 427-437.

31 Podolin PL, Callahan JF, Bolognese BJ, Li YH, Carlson K, Davis TG *et al*. Attenuation of murine collagen-induced arthritis by a novel, potent, selective small molecule inhibitor of IkappaB Kinase 2, TPCA-1 (2-[(aminocarbonyl)amino]-5-(4-fluorophenyl)-3-thiophenecarboxamide), occurs via reduction of proinflammatory cytokines and antigen-induced T cell Proliferation. *J Pharmacol Exp Ther* 2005; 312: 373-381.

32 Blackford AN, Jackson SP. ATM, ATR, and DNA-PK: The Trinity at the Heart of the DNA Damage Response. *Mol Cell* 2017; 66: 801-817.

33 Hadian K, Krappmann D. Signals from the nucleus: activation of NF-kappaB by cytosolic ATM in the DNA damage response. *Sci Signal* 2011; 4: pe2.

34 Liu L, Kwak YT, Bex F, Garcia-Martinez LF, Li XH, Meek K *et al*. DNA-dependent protein kinase phosphorylation of IkappaB alpha and IkappaB beta regulates NF-kappaB DNA binding properties. *Mol Cell Biol* 1998; 18: 4221-4234.

35 Bozulic L, Surucu B, Hynx D, Hemmings BA. PKBalpha/Akt1 acts downstream of DNA-PK in the DNA double-strand break response and promotes survival. *Mol Cell* 2008; 30: 203-213.

36 Oeckinghaus A, Hayden MS, Ghosh S. Crosstalk in NF-kappaB signaling pathways. *Nat Immunol* 2011; 12: 695-708.

37 Gavande NS, VanderVere-Carozza PS, Hinshaw HD, Jalal SI, Sears CR, Pawelczak KS *et al*. DNA repair targeted therapy: The past or future of cancer treatment? *Pharmacol Ther* 2016; 160: 65-83.

38 Peng Y, Woods RG, Beamish H, Ye R, Lees-Miller SP, Lavin MF *et al*. Deficiency in the catalytic subunit of DNA-dependent protein kinase causes down-regulation of ATM. *Cancer Res* 2005; 65: 1670-1677.

39 Hong SP, Chan TE, Lombardo Y, Corleone G, Rotmensz N, Bravaccini S *et al*. Single-cell transcriptomics reveals multi-step adaptations to endocrine therapy. *Nature communications* 2019; 10: 3840.

40 Gadducci A, Guarneri V, Peccatori FA, Ronzino G, Scandurra G, Zamagni C *et al*. Current strategies for the targeted treatment of high-grade serous epithelial ovarian cancer and relevance of BRCA mutational status. *J Ovarian Res* 2019; 12: 9.

41 Stronach EA, Chen M, Maginn EN, Agarwal R, Mills GB, Wasan H *et al*. DNA-PK mediates AKT activation and apoptosis inhibition in clinically acquired platinum resistance. *Neoplasia* 2011; 13: 1069-1080.

42 Langdon SP, Lawrie SS, Hay FG, Hawkes MM, McDonald A, Hayward IP *et al*. Characterization and properties of nine human ovarian adenocarcinoma cell lines. *Cancer Res* 1988; 48: 6166-6172.

43 Basu S, Rosenzweig KR, Youmell M, Price BD. The DNA-dependent protein kinase participates in the activation of NF kappa B following DNA damage. *Biochem Biophys Res Commun* 1998; 247: 79-83.

44 Panta GR, Kaur S, Cavin LG, Cortes ML, Mercurio F, Lothstein L *et al*. ATM and the catalytic subunit of DNA-dependent protein kinase activate NF-kappaB through a common MEK/extracellular signal-regulated kinase/p90(rsk) signaling pathway in response to distinct forms of DNA damage. *Mol Cell Biol* 2004; 24: 1823-1835.

45 Sabatel H, Pirlot C, Piette J, Habraken Y. Importance of PIKKs in NF-kappaB activation by genotoxic stress. *Biochem Pharmacol* 2011; 82: 1371-1383.

46 Fang Y, Chai Z, Wang D, Kuang T, Wu W, Lou W. DNA-PKcs deficiency sensitizes the human hepatoma HepG2 cells to cisplatin and 5-fluorouracil through suppression of the PI3K/Akt/NF-kappaB pathway. *Mol Cell Biochem* 2015; 399: 269-278.

47 Rajagopalan S, Moyle MW, Joosten I, Long EO. DNA-PKcs controls an endosomal signaling pathway for a proinflammatory response by natural killer cells. *Sci Signal* 2010; 3: ra14.

48 Faltas BM, Prandi D, Tagawa ST, Molina AM, Nanus DM, Sternberg C *et al*. Clonal evolution of chemotherapy-resistant urothelial carcinoma. *Nat Genet* 2016; 48: 1490-1499.

49 Jamal-Hanjani M, Wilson GA, McGranahan N, Birkbak NJ, Watkins TBK, Veeriah S *et al*. Tracking the Evolution of Non-Small-Cell Lung Cancer. *N Engl J Med* 2017; 376: 2109-2121.

50 Treiber T, Treiber N, Plessmann U, Harlander S, Daiss JL, Eichner N *et al*. A Compendium of RNA-Binding Proteins that Regulate MicroRNA Biogenesis. *Mol Cell* 2017; 66: 270-284 e213.

51 Nik-Zainal S, Wedge DC, Alexandrov LB, Petljak M, Butler AP, Bolli N *et al*. Association of a germline copy number polymorphism of APOBEC3A and APOBEC3B with burden of putative APOBEC-dependent mutations in breast cancer. *Nat Genet* 2014; 46: 487-491.

52 Zaky A, Busso C, Izumi T, Chattopadhyay R, Bassiouny A, Mitra S *et al*. Regulation of the human AP-endonuclease (APE1/Ref-1) expression by the tumor suppressor p53 in response to DNA damage. *Nucleic acids research* 2008; 36: 1555-1566.

53 Serebrenik AA, Argyris PP, Jarvis MC, Brown WL, Bazzaro M, Vogel RI *et al*. The DNA Cytosine Deaminase APOBEC3B is a Molecular Determinant of Platinum Responsiveness in Clear Cell Ovarian Cancer. *Clinical cancer research : an official journal of the American Association for Cancer Research* 2020; 26: 3397-3407.

54 Leonard B, Starrett GJ, Maurer MJ, Oberg AL, Van Bockstal M, Van Dorpe J *et al*. APOBEC3G Expression Correlates with T-Cell Infiltration and Improved Clinical Outcomes in High-grade Serous Ovarian Carcinoma. *Clinical cancer research : an official journal of the American Association for Cancer Research* 2016; 22: 4746-4755.

55 Sur S, Pagliarini R, Bunz F, Rago C, Diaz LA, Jr., Kinzler KW *et al*. A panel of isogenic human cancer cells suggests a therapeutic approach for cancers with inactivated p53. *Proc Natl Acad Sci U S A* 2009; 106: 3964-3969.

56 Ding Q, Regan SN, Xia Y, Oostrom LA, Cowan CA, Musunuru K. Enhanced efficiency of human pluripotent stem cell genome editing through replacing TALENs with CRISPRs. *Cell Stem Cell* 2013; 12: 393-394.

57 Curtis C, Shah SP, Chin SF, Turashvili G, Rueda OM, Dunning MJ *et al*. The genomic and transcriptomic architecture of 2,000 breast tumours reveals novel subgroups. *Nature* 2012; 486: 346-352.

58 Schneider CA, Rasband WS, Eliceiri KW. NIH Image to ImageJ: 25 years of image analysis. *Nat Methods* 2012; 9: 671-675.

Figure Legends

Figure 1. APOBEC3B expression is associated with poor patient response to chemotherapy in breast cancer. (**A-B**) KM plot of breast cancer patients from microarray data sets (A; GEO series) and METABRIC (B), only including patients who were reported to have been treated with chemotherapy. (**C-D**) A3B expression is lower in estrogen receptor-positive breast cancer patients who responded to chemotherapy than in patients who did not respond. P-values were generated using the Mann-Whitney U test. The GEO series includes sample with follow-up data from the gene expression microarray data sets GSE1456, GSE16391, GSE16446, GSE16716, GSE17907, GSE19615, GSE20271, GSE21653, GSE31519, GSE3494, GSE37946, GSE45255, GSE4611, GSE5327 and GSE69031. (**E**) Clonogenic assays were performed for MCF7 and MCF7-A3B$^{-/-}$ cells in the presence of the drugs at seven concentrations, ranging between 0.001 - 10 μM (cisplatin, etoposide, 5-FU), or 0.01 - 100 nM (doxorubicin, SN-38). The graphs plot IC_{50} values for 4 independent experiments. (**F**) Immunoblotting was performed using protein lysates prepared 24 hours following addition of Cisplatin (20 μM), Etoposide (10 μM), 5-FU (50 μM), doxorubicin (100 nM), or SN-38 (50 nM) to MCF7 and MCF7-A3B$^{-/-}$ cells.

Figure 2. Cancer chemotherapy drugs promote APOBEC3B expression in a p53-independent manner. (**A, B**) RNA and protein lysates were prepared 24 hours following drug addition to HCT116 and p53-null HCT116 cells. RT-qPCR is shown relative to GAPDH levels (n=3). Significantly ($p<0.05$) higher (*) or lower (#) gene expression, relative to the vehicle control, are indicated. (**C**) p53 ChIP following addition of Nutlin3, etoposide or cisplatin for 24 hours to HCT116 cells (n=3). The NEU3 promoter region was identified as a negative control for p53 binding from analysis of p53 ChIP-seq data [19]. (**D**) Genome browser snapshot of human chromosome 22 region encoding APOBEC3 genes, with p53 ChIP-seq data for HCT116 cells treated for 12 hours with 10 μM Nutlin3, downloaded from NCBI GEO (GSE86222) [19].

Figure 3. Chemotherapeutic drugs stimulate A3B cytidine deaminase activity in cancer cells. (**A-D**) Protein lysates prepared from cell lines treated with drugs for 24 hours, were

used in the cytidine deaminase assay. Positions of the substrate (probe) and the deamination product, are labelled. CAL51 are WT for p53, T47D and MDA-MB-453 express mutant p53. Levels of the deaminase product were quantified using densitometric analysis using Image J [58]. The results of three independent experiments are shown in the bar charts, including the individual values (circles). Asterisks represent statistically significant ($p<0.05$; n=3) differences in deaminase products for drug-treated samples, relative to vehicle controls. (**E, F, G**) AP sites in genomic DNA from indicated cell lines treated with drugs for 24 hours, were quantified by AP site conversion with a biotinylated aldehyde reactive probe and quantification of biotinylated DNA. Asterisks show statistically significant ($p<0.05$; n=3) differences in AP sites for drug-treated samples, relative to vehicle controls.

Figure 4. NF-κB mediates induction of APOBEC3B gene expression by chemotherapy drugs. (**A-C**) Bar graphs show ChIP-qPCR enrichment for transcription factors or the H3K27ac mark, for ChIP lysates prepared 24 hours following addition of drugs, as fold enrichment relative to vehicle-treated cells. Asterisks show significant ($p<0.05$) differences in factor enrichment relative to the vehicle control for each of the two cell lines. (**D**) ChIP was performed following addition of drugs ± NF-κB inhibitors BAY 11-7208 (BAY) or TPCA-1 (n=3; * = $p<0.05$). (**E, F**) RNA and protein lysates prepared from T47D cells, 24 hours following drug addition, were used for RT-qPCR and immunoblotting, respectively. RT-qPCR results were normalised for GAPDH expression (n=3). Statistically significant reductions in A3B expression, for NF-κB inhibitor-treated samples, compared to the expression for each chemotherapy drug, are marked by asterisks ($p<0.05$).

Figure 5. Stimulation of APOBEC3B expression is promoted by DNA-PK directed NF-κB activation. (**A**) Pathway from DNA damaging chemotherapy drugs to NF-κB stimulation of A3B expression. (**B**) RT-qPCR using RNA prepared from T47D cells treated with increasing concentrations of the DNA-PKcs inhibitor, NU7441, for 24 hours. Asterisks highlight significant ($p<0.05$; n=3) differences relative to vehicle treatment. (**C**) T47D cells were treated with cisplatin or etoposide ± 5 μM NU7441, for 24 hours. Asterisks denote statistically significant differences in A3B expression, when comparing the NU7441-treated samples with corresponding samples not treated with NU7441 ($p<0.05$; n=3). (**D**)

Immunoblotting of T47D cell lysates following treatment with cisplatin or etoposide ± 5 μM NU7441. (**E**) T47D cells were transfected with siRNA for DNA-PKcs (siDNA-PK) or a control siRNA (siControl). Cisplatin or etoposide were added 24 hours following transfection and protein lysates prepared after a further 24 hours. (**F, G**) Protein lysates from T47D cells treated with cisplatin or etoposide for ± DNA-PKcs (NU7441), ATM (KU55933), AKT (MK2206) or NF-κB (BAY-11-7082, TPCA1) inhibitors for 24 hours, were used in the cytidine deaminase assay. Densitometric quantification of deaminase products using Image J (n=3 independent experiments), is shown in the bar charts. Asterisks show statistically significant ($p<0.05$) differences in deaminase products for inhibitor-treated samples, relative to the cisplatin- or etoposide-treated samples. The circles show values for each sample and error bars = standard errors of the mean.

Figure 6. The DNA-PKcs/AKT/NF-κB axis is constitutively active and APOBEC3B expression is increased in cisplatin-resistant ovarian cancer cells. (**A**) RT-qPCR using RNA prepared from PEA1 and PEA2 ovarian cancer cells for A3B and NF-κB target genes. (**B**) Immunoblotting of PEA1 and PEA2 protein lysates. (**C**) Cytidine deaminase assay performed with lysates prepared from PEA1 and PEA2 cells. Protein lysate was omitted in the no lysate control. The bar chart shows the results of three independent experiments. Cytidine deaminase activity was significantly different between PEA1 and PEA2 cells (* = $p<0.05$). (**D**) ChIP-qPCR enrichment for NF-κB proteins in PEA1 and PEA2 cells. (**E**) Protein lysates prepared 24 hours following drug treatment of PEA2 cells were used for immunoblotting. (**F**) PEA1 and PEA2 cells were transfected with A3B or control siRNA. Cisplatin was added 24 hours following transfection at concentrations ranging from 0.8 nM to 50 μM (4-fold serial dilutions). Growth was determined using the SRB assay after a further 48 hours. IC_{50} values for 4 independent experiments are plotted. The graph on the right shows A3B expression relative to expression of GAPDH. (**G, H**) Cisplatin (20 μM) was added as in (F) and cell lysates were assessed for caspase 3/7 activity (n=3) or immunoblotted, as shown.

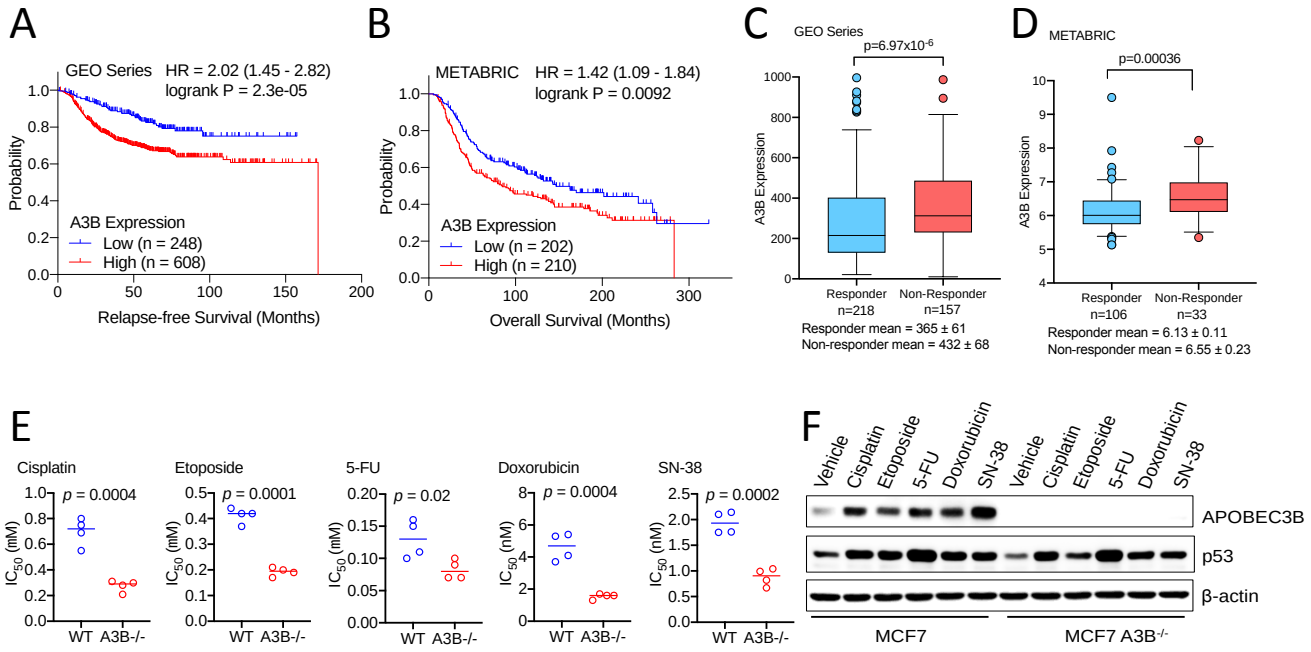

A
GEO Series HR = 2.02 (1.45 - 2.82)
logrank P = 2.3e-05
Probability
A3B Expression
Low (n = 248)
High (n = 608)
Relapse-free Survival (Months)
B
METABRIC HR = 1.42 (1.09 - 1.84)
logrank P = 0.0092
Probability
A3B Expression
Low (n = 202)
High (n = 210)
Overall Survival (Months)
C
GEO Series
p=6.97x10-6
A3B Expression
Responder n=218
Non-Responder n=157
Responder mean = 365 ± 61
Non-responder mean = 432 ± 68
D
METABRIC
p=0.00036
A3B Expression
Responder n=106
Non-Responder n=33
Responder mean = 6.13 ± 0.11
Non-responder mean = 6.55 ± 0.23
E
Cisplatin
p = 0.0004
Etoposide
p = 0.0001
5-FU
p = 0.02
Doxorubicin
p = 0.0004
SN-38
p = 0.0002
IC50 (mM)
IC50 (nM)
WT
A3B-/-
F
Vehicle
Cisplatin
Etoposide
5-FU
Doxorubicin
SN-38
APOBEC3B
p53
β-actin
MCF7
MCF7 A3B-/-

Figure 1

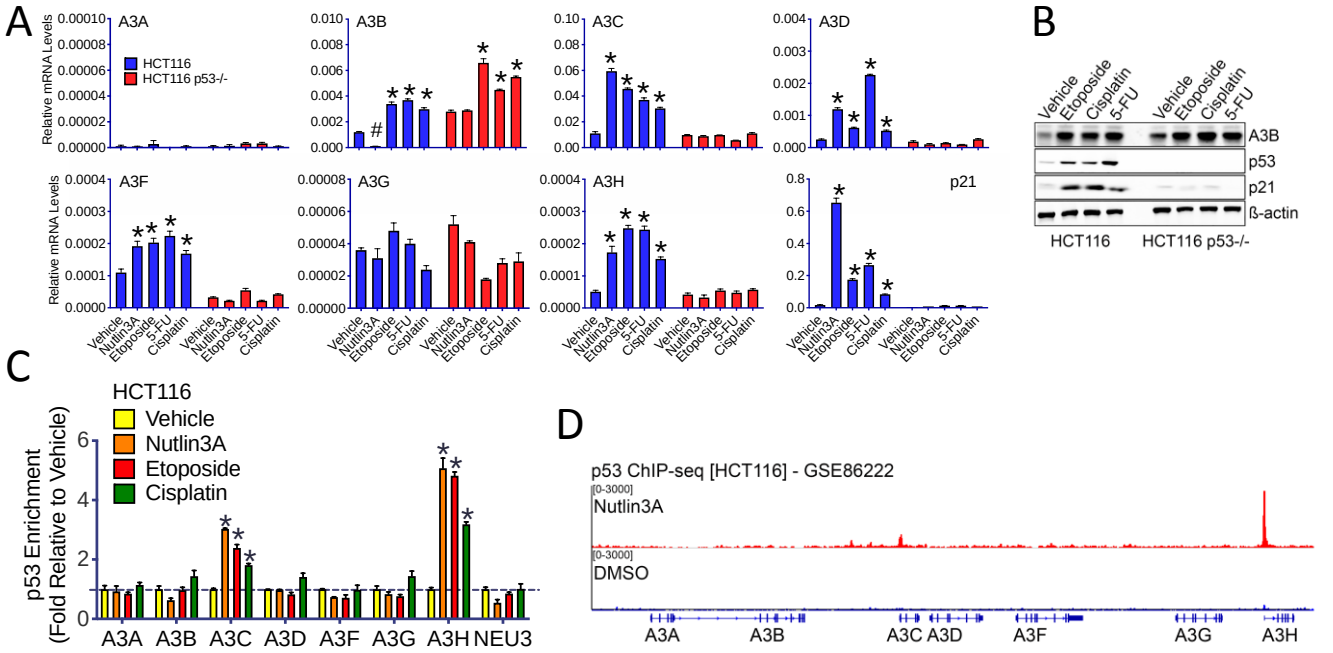

A
Relative mRNA Levels
A3A
HCT116
HCT116 p53-/-
A3B
A3C
A3D
A3F
A3G
A3H
p21
Vehicle
Nutlin3A
Etoposide
5-FU
Cisplatin
B
Vehicle
Etoposide
Cisplatin
5-FU
A3B
p53
p21
ß-actin
HCT116
HCT116 p53-/-
C
HCT116
Vehicle
Nutlin3A
Etoposide
Cisplatin
p53 Enrichment
(Fold Relative to Vehicle)
A3A A3B A3C A3D A3F A3G A3H NEU3
D
p53 ChIP-seq [HCT116] - GSE86222
[0-3000]
Nutlin3A
[0-3000]
DMSO
A3A A3B A3C A3D A3F A3G A3H

Figure 2

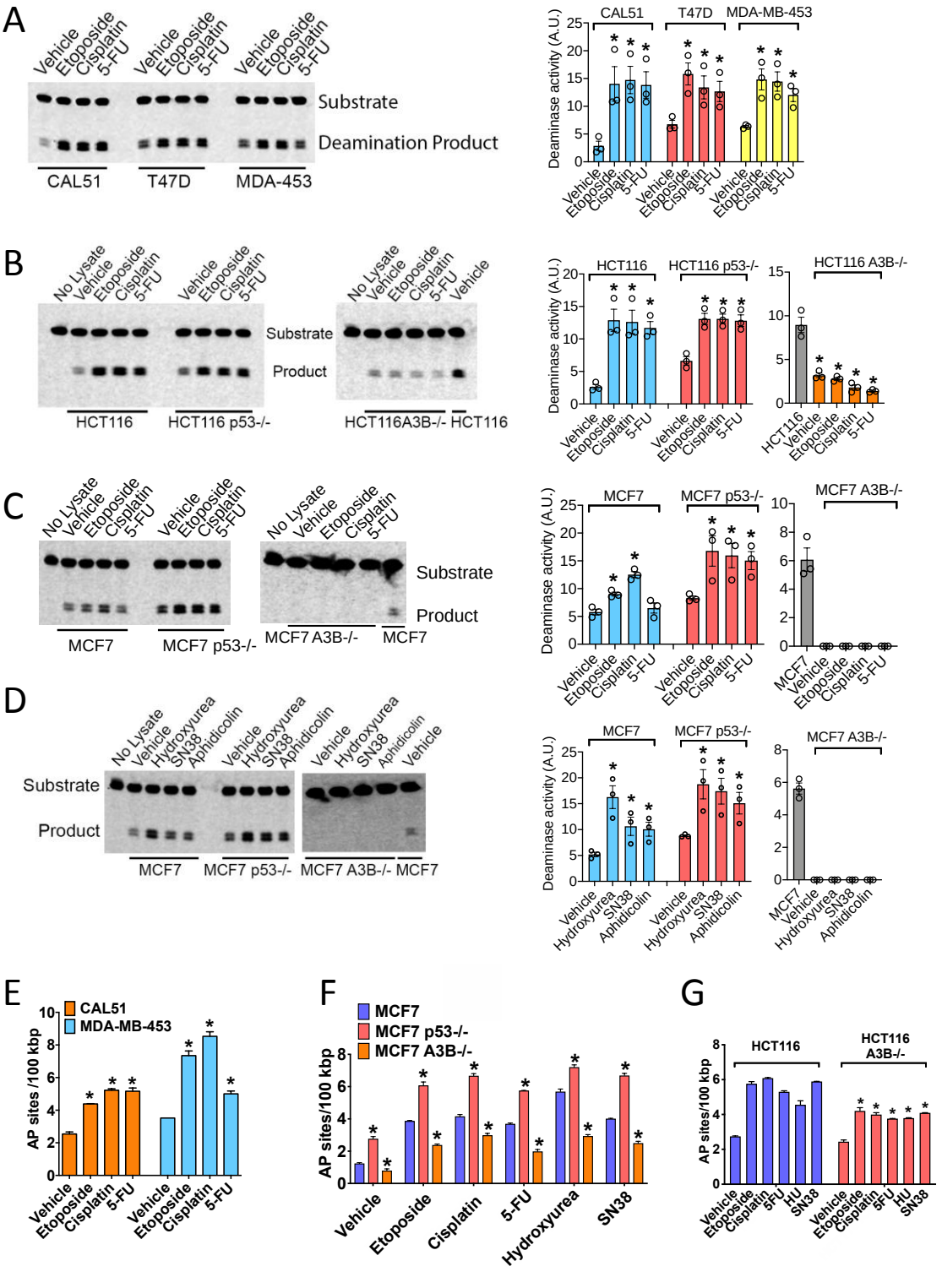

A
Vehicle
Etoposide
Cisplatin
5-FU
Substrate
Deamination Product
CAL51
T47D
MDA-453
Deaminase activity (A.U.)
B
No Lysate
HCT116
HCT116 p53-/-
HCT116A3B-/-
HCT116 A3B-/-
C
MCF7
MCF7 p53-/-
MCF7 A3B-/-
D
Hydroxyurea
SN38
Aphidicolin
E
AP sites /100 kbp
F
G
HU

Figure 3

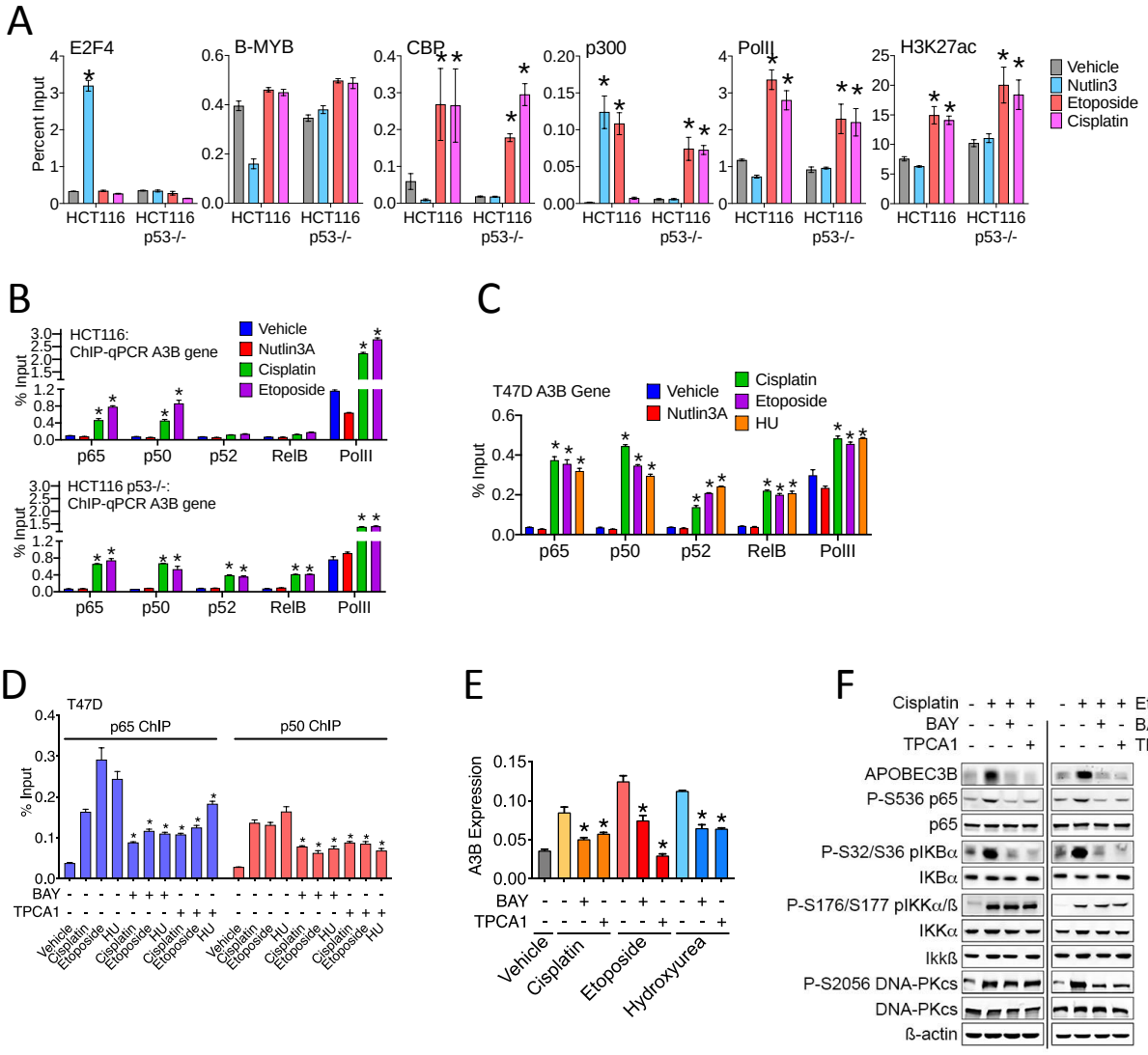

A
E2F4
B-MYB
CBP
p300
PolII
H3K27ac
Percent Input
HCT116
HCT116 p53-/-
Vehicle
Nutlin3
Etoposide
Cisplatin
B
HCT116:
ChIP-qPCR A3B gene
HCT116 p53-/-:
% Input
p65
p50
p52
RelB
PolII
C
T47D A3B Gene
HU
D
T47D
p65 ChIP
p50 ChIP
BAY
TPCA1
E
A3B Expression
Hydroxyurea
F
Cisplatin
Etoposide
APOBEC3B
P-S536 p65
p65
P-S32/S36 pIKBα
IKBα
P-S176/S177 pIKKα/ß
IKKα
Ikkß
P-S2056 DNA-PKcs
DNA-PKcs
ß-actin

Figure 4

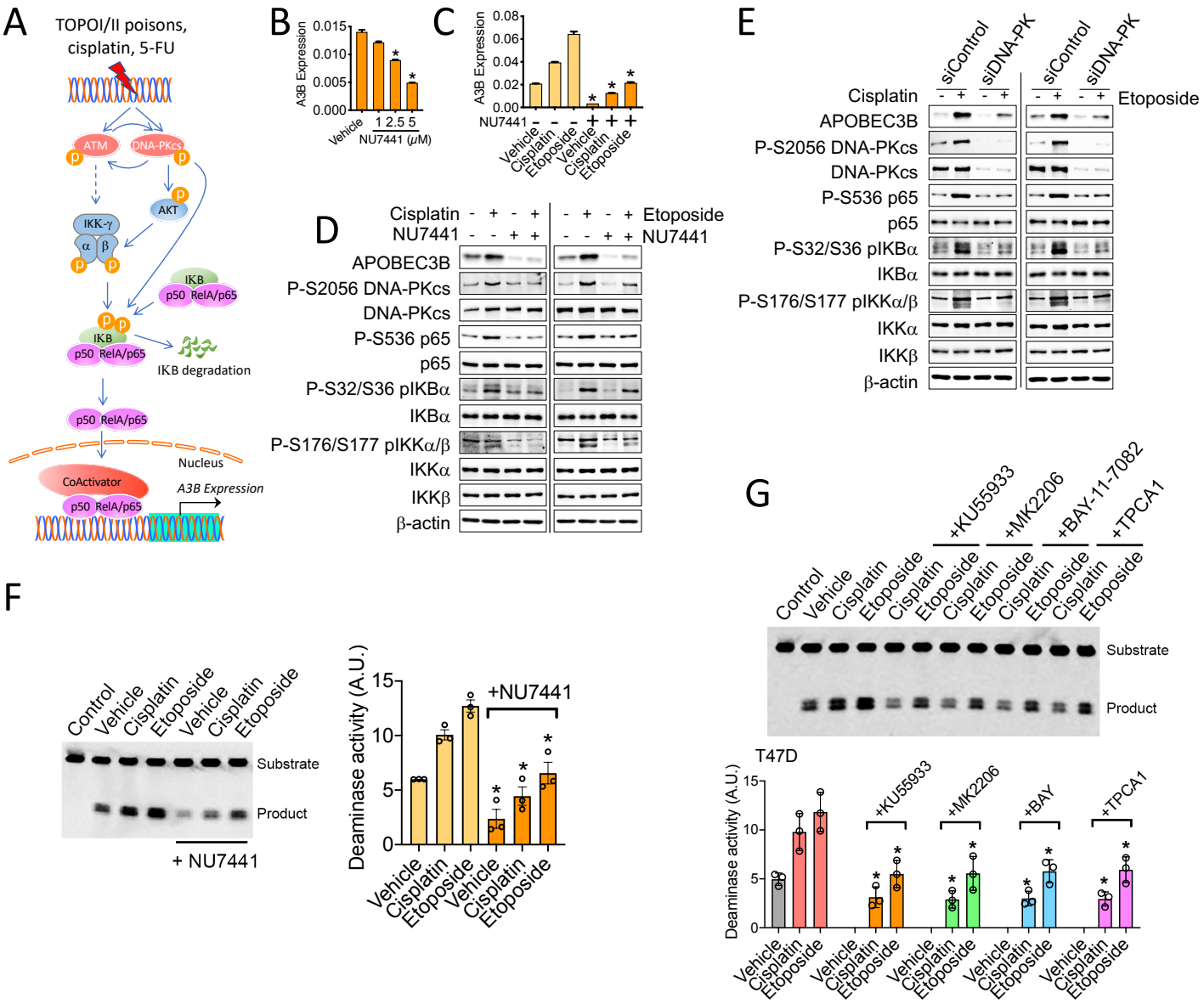

A
TOPOI/II poisons, cisplatin, 5-FU
ATM
DNA-PKcs
AKT
IKK-γ
IKB
p50 RelA/p65
IKB degradation
Nucleus
CoActivator
A3B Expression
B
A3B Expression
Vehicle
1 2.5 5
NU7441 (μM)
C
A3B Expression
NU7441
Vehicle
Cisplatin
Etoposide
D
Cisplatin
NU7441
Etoposide
APOBEC3B
P-S2056 DNA-PKcs
DNA-PKcs
P-S536 p65
p65
P-S32/S36 pIKBα
IKBα
P-S176/S177 pIKKα/β
IKKα
IKKβ
β-actin
E
siControl
siDNA-PK
Cisplatin
Etoposide
APOBEC3B
P-S2056 DNA-PKcs
DNA-PKcs
P-S536 p65
p65
P-S32/S36 pIKBα
IKBα
P-S176/S177 pIKKα/β
IKKα
IKKβ
β-actin
F
Control
Vehicle
Cisplatin
Etoposide
Substrate
Product
+ NU7441
Deaminase activity (A.U.)
+NU7441
G
+KU55933
+MK2206
+BAY-11-7082
+TPCA1
Substrate
Product
T47D
Deaminase activity (A.U.)
+BAY

Figure 5

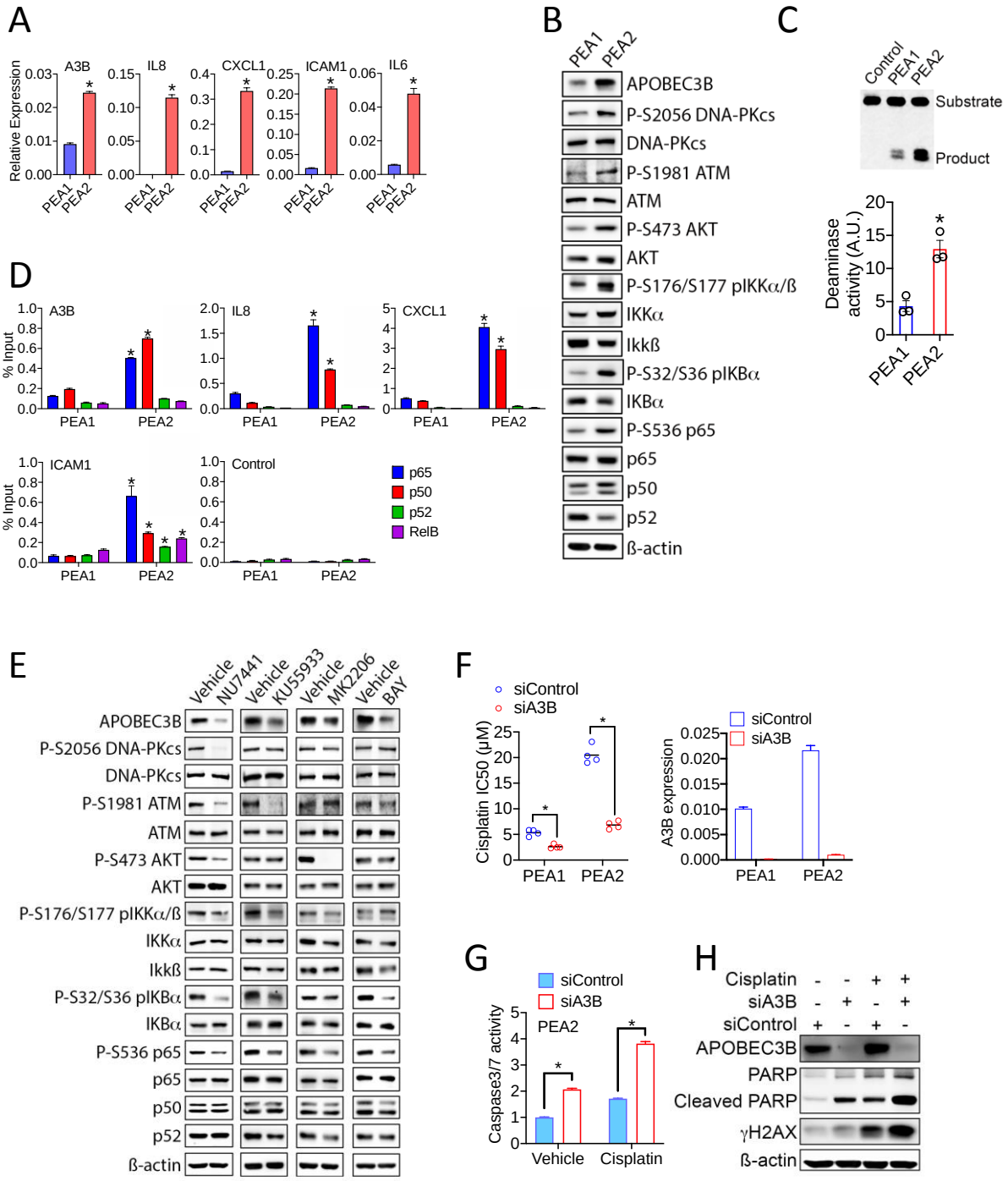

A
A3B
IL8
CXCL1
ICAM1
IL6
Relative Expression
PEA1
PEA2
B
PEA1
PEA2
APOBEC3B
P-S2056 DNA-PKcs
DNA-PKcs
P-S1981 ATM
ATM
P-S473 AKT
AKT
P-S176/S177 pIKKα/ß
IKKα
Ikkß
P-S32/S36 pIKBα
IKBα
P-S536 p65
p65
p50
p52
ß-actin
C
Control
PEA1
PEA2
Substrate
Product
Deaminase activity (A.U.)
D
A3B
IL8
CXCL1
ICAM1
Control
% Input
p65
p50
p52
RelB
E
Vehicle
NU7441
KU55933
MK2206
BAY
F
siControl
siA3B
Cisplatin IC50 (μM)
A3B expression
G
Caspase3/7 activity
Vehicle
Cisplatin
H
Cisplatin
siA3B
siControl
APOBEC3B
PARP
Cleaved PARP
γH2AX
ß-actin

Figure 6

Supplementary Table 1. Drugs

Compound	Cat. No.	Supplier	Final Concn.
Nutlin-3a (Nutlin)	3984	Tocris	10 μM
Etoposide	E1383	Sigma	10 μM
5-fluorouracil (5-FU)	F6627	Sigma	50 μM
Cisplatin	2251	Tocris	20 μM
Hydroxyurea (HU)	H2687	Sigma	2 mM
SN38	2684	Tocris	50 nM
Aphidicolin	5736	Tocris	400 μM
NU7441	3712	Tocris	5 μM
KU55933	3544	Tocris	5 μM
VE-821	6160	Tocris	5 μM
MK2206	S1078-SEL	Stratech Scientific	5 μM
BAY 11-7082 (BAY)	196870	Calbiochem	10 μM
TPCA-1	2559	Tocris	5 μM

Supplementary Table 2. Antibodies for ChIP

Antibody	Cat. No.	Supplier	Antibody (μg)
p53	sc-126	Santa Cruz Biotechnology	5
E2F4	sc-866	Santa Cruz Biotechnology	5
p130	sc-317	Santa Cruz Biotechnology	5
KDM5A	A300-897A	Bethyl Laboratories Inc.	5
p300	sc-584	Santa Cruz Biotechnology	5
CBP	sc-7300	Santa Cruz Biotechnology	10
B-MYB	sc-724	Santa Cruz Biotechnology	5
RNA Polymerase II (PolII)	sc-47701	Santa Cruz Biotechnology	5
H3K27ac	ab4729	Abcam	5
DNA-PKcs	sc-9051	Santa Cruz Biotechnology	5
RelA/p65	8242s	Cell signaling technology	10
p50	13586s	Cell signaling technology	10
p52	37359s	Cell signaling technology	10
RelB	10544s	Cell signaling technology	10

Supplementary Table 3. Taqman Gene Expression Assays (ABI Thermofisher, UK)

Gene	Cat. No.
APOBEC3A	Hs00377444
APOBEC3B	Hs00358981
APOBEC3C	Hs00828074
APOBEC3D	Hs00537163
APOBEC3F	Hs01665324
APOBEC3G	Hs00222415
APOBEC3H	Hs00419665
CDKN1A (p21)	Hs00355782
ICAM1	Hs00164932
IL8	Hs00174103
CXCL1	Hs00236937
GAPDH	Hs99999905

Supplementary Table 4. siRNA (Dharmacon,UK)

Gene	Cat. No.
APOBEC3B	L-017322-00-0005
NFKB1	L-003520-00-0005
NFKB2	L-003918-00-0005
RELA	L-003533-00-0005
ATM	L-003201-00-0005
ATR	003202-00-0005

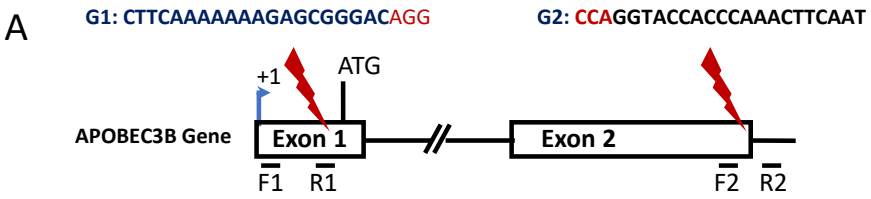
Supplementary Table 5. ChIP-qPCR Primer sequences

Gene Promoter	Forward and Reverse primer sequences
APOBEC3A	5’-AGAGTGGGCACATCAAAACC-3’ 5’-AACCTGGAAGCTGCTGAGTC-3’
APOBEC3B	5’-GGTCACTTTAAGGAGGGCTGT-3’ 5’-TAGATACGCTTGTCCCTGTCC-3’
APOBEC3C	5’-AACCAGAAAGAGGGCCAGAG-3’ 5’-TTACAGCGTCCTTGCAGTTG-3’
APOBEC3D	5’-CCTACACCAGCGCCTGAG-3’ 5’-GTGAGAGAGCGAGGCTTCC-3’
APOBEC3F	5’-CAGACACCTGGCCCTTTACT-3’ 5’-CCTCCTCTCCACCATCAAGA-3’
APOBEC3G	5’-AGACGCCTGGCCATTTACT-3’ 5’-CCTCCTCTCCACCATCAAGA-3’
APOBEC3H	5’-CTCCAGTCCCACAAAAGGAA-3’ 5’-TTCACTTTTGGCAGCTCTCC-3’
CDKN1A (p21)	5’-CTCCATCCCTATGCTGCCTG-3’ 5’-AGGCAGCCCAAGGACAAAAT-3’
MDM2	5’-GTTCAGTGGGCAGGTTGACT-3’, 5’-CACTGAACACAGCTGGGAAA-3’
ICAM1	5’-ACCGTGATTCAAGCTTAGCC-3’ 5’-GCTGCAGTTATTTCCGGACT-3’
IL8	5’-AAGTGTGATGACTCAGGTTTGC-3’ 5’-TTTGTGCCTTATGGAGTGCT-3’
CXCL1	5’-AACCATGCATAAAAGGGGTTC-3’ 5’-GTCTGGCGGCTGTGAGAG-3’
CNTNAP5 (negative control)	5’-TCTCACCTCACTGCAACCAC-3’ 5’-TAGTTGGGCATGGTGTCTCA-3’
NEU3 (negative control)	5’-TCTTTTCGTTGCCGTTACCT-3’ 5’-TGGGGAGACTGAGACAGAGG-3’

Supplementary Table 6. Antibodies for Immunoblotting

Antibody	Cat. No.	Supplier	Antibody Dilution
p53	sc-126	Santa Cruz Biotechnology	1:1000
CDKN1A (p21)	sc-397	Santa Cruz Biotechnology	1:500
APOBEC3B	ab184990	Abcam	1:500
DNA-PKcs (P-Ser2056)	ab18192	Abcam	1:1000
DNA-PKcs	sc-9051	Santa Cruz Biotechnology	1:1000
RelA/p65 (P-Ser536)	3033s	Cell signaling technology	1:1000
RelA/p65	8242s	Cell signaling technology	1:1000
IKBα (P-Ser32/P-Ser36)	9246s	Cell signaling technology	1:1000
IKKα/ß (P-Ser176/P-Ser177)	2078s	Cell signaling technology	1:1000
IKKα	11930s	Cell signaling technology	1:1000
IKKß	8943s	Cell signaling technology	1:1000
AKT	9272s	Cell signaling technology	1:1000
pAKT (P-Ser473)	9271s	Cell signaling technology	1:1000
ATM	2873s	Cell signaling technology	1:1000
pATM (P-Ser1981)	4526s	Cell signaling technology	1:1000
p50 (NFKB1)	13586s	Cell signaling technology	1:1000
p52 (NFKB2)	37359s	Cell signaling technology	1:1000
ß-actin	ab6276	Abcam	1:50000
PARP	9532S	Cell signaling technology	1:1000
γH2AX (S139)	05-636	Millipore	1:1000

Supplemental Information: generation of A3B knockout MCF7 and HCT116 cell lines



F1: gccctgggaggtcactttaag
R1: cctgctgggcctcaaccct
F2: ggagtgggttggcagaaata
R2: gatatgggtgagacaggagga

B

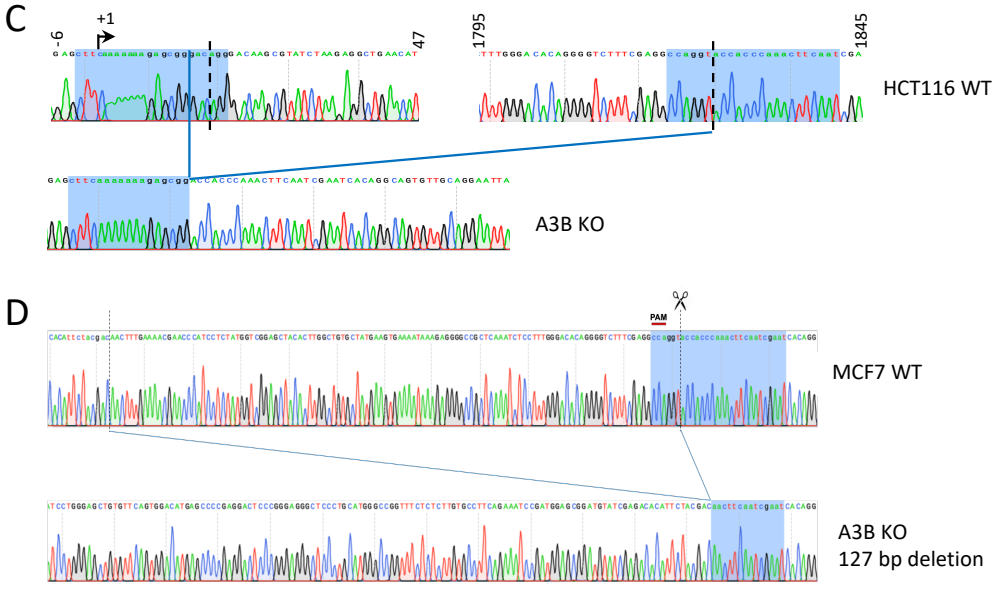
A3B gBlock 1

TGTACAAAAAAGCAGGCTTTAAAGGAACCAATTCAGTCGACTGGATCCGGTACCAAGGTCGGGCAGGAAGAGGGCCTATTTCCCATGATTC
CTTCATATTTGCATATACGATACAAGGCTGTTAGAGAGATAATTAGAATTAATTTGACTGTAAACACAAAGATATTAGTACAAAATACGTGA
CGTAGAAAGTAATAATTTCTTGGGTAGTTTGCAGTTTTAAAATTATGTTTTAAAATGGACTATCATATGCTTACCGTAACTTGAAAGTATTTC
GATTTCTTGGCTTTATATATCTTGTGGAAAGGACGAAACACCGTTCAAAAAAAGAGCGGGACGTTTTAGAGCTAGAAATAGCAAGTTAAAA
TAAGGCTAGTCCGTTATCAACTTGAAAAAGTGGCACCGAGTCGGTGCTTTTTTTCTAGACCCAGCTTTCTTGTACAAAGTTGGCATTA

A3B gBlock 2

TGTACAAAAAAGCAGGCTTTAAAGGAACCAATTCAGTCGACTGGATCCGGTACCAAGGTCGGGCAGGAAGAGGGCCTATTTCCCATGATTC
CTTCATATTTGCATATACGATACAAGGCTGTTAGAGAGATAATTAGAATTAATTTGACTGTAAACACAAAGATATTAGTACAAAATACGTGA
CGTAGAAAGTAATAATTTCTTGGGTAGTTTGCAGTTTTAAAATTATGTTTTAAAATGGACTATCATATGCTTACCGTAACTTGAAAGTATTTC
GATTTCTTGGCTTTATATATCTTGTGGAAAGGACGAAACACCGTTGAAGTTTGGGTGGTACCGTTTTAGAGCTAGAAATAGCAAGTTAAAAT
AAGGCTAGTCCGTTATCAACTTGAAAAAGTGGCACCGAGTCGGTGCTTTTTTTCTAGACCCAGCTTTCTTGTACAAAGTTGGCATTA

Black: U6 Promoter
Green: A3B guide RNA sequence
Red: guide RNA scaffold
Blue: transcription termination sequence



(A) Schematic of the A3B gene showing positions and sequences of the guide RNAs, with PAM sequences shown in red. Also shown are the sequences of primers used for amplification and sequencing of the region. Both guide RNAs were used in HCT116, whereas only guide RNA 2 was used in MCF7 cells. gBlock gene fragments encoding the U6 promoter, guide RNA sequence targeting exon 1 or the exon 2/intron 2 boundary of the A3B gene, guide RNA scaffold and transcription termination signal were synthesised by Integrated DNA

Technologies (Belgium). The gblock gene fragments were PCR amplified and cloned into pCR2.1-TA (Thermofisher, UK). Cells were co-transfected with the *pCAG*-Cas9-2A-GFP vector and the gBlock plasmids. 48 hrs post-transfection, GFP-positive cells were isolated by FACS and single cells were cultured in 96-well plates. Following expansion of single cells, genomic DNA was prepared using the Blood & Cell Culture DNA Mini Kit (Qiagen, UK). The clones were screened by PCR and A3B deletion was confirmed by DNA sequencing and immunoblotting. (B) Sequences of the two gblock gene fragments synthesised for cloning into pCR2.1-TA are shown. (C, D) Sanger sequencing of HCT116, MCF7 and the A3B KO clones used in this study, are shown.

Supplementary Figure Legends

Supplementary Figure 1. **APOBEC3B expression is associated with poor patient response to chemotherapy in breast cancer.** (**A**) KM plot of breast cancer patients from microarray data sets, including only patients who were treated with chemotherapy. The results in this plot are also shown in Figure 1A, but here include details of patient numbers. (**B**) KM plot of ER+ breast cancer patients from microarray data sets, including patients who were treated with chemotherapy, but excluding those patients who received hormone therapy.

Supplementary Figure 2. Chemotherapeutic agents promote APOBEC3B expression in a p53-independent manner. (**A**) Heat map shows that expression of A3B is stimulated by etoposide, 5-fluorouracil (5-FU) and cisplatin in cancer cell lines wild-type for p53 (MCF7, CAL51, ZR-75-1), expressing mutant p53 (T47D, MDA-MB-453), or in p53-WT and p53-null HCT116. A3B expression is shown as fold relative to the vehicle control for each cell line (n=3). (**B**) Immunoblotting of p53 wild-type and mutant cells using lysates prepared 24 hours following addition of drug. (**C**) Total RNA prepared from HCT116 and HCT116 p53-/- cells treated with hydroxyurea (HU), SN38 or with aphidicolin for 24 hours, was used for RT-qPCR analysis of APOBEC3 genes. RT-qPCR for p21 serves as a marker for p53 activation. Expression of the genes is shown relative to expression of GAPDH. Asterisks mark statistically significant ($p<0.05$; n=3) difference in expression relative to the vehicle control. (**D**) MCF7 and p53-null MCF7 were treated with the indicated drugs for 24 hours. Total RNAs were used in RT-qPCR. As previously, gene expression is shown relative to expression of GAPDH. Asterisks show statistically significant ($p<0.05$; n=3) difference in A3B or p21 expression, relative to expression in the appropriate vehicle control. **(E)** Immunoblotting of MCF7 WT, MCF7 p53-null and MCF7 A3B-null cells for A3B, p53 and ß-actin. **(F)** Immunoblotting of lysates prepared from HCT116 WT, HCT116 p53-null and HCT116 A3B-null cells. (**G**) RT-qPCR (n=3) for APOBEC3 genes, normalised to GAPDH expression, comparing MCF7 cells with A3B-null MCF7 cells. Cells were treated with the drugs for 24 hours.

Supplementary Figure 3. ChIP analysis shows chemotherapy drug enrichment of NF-κB at the APOBEC3B gene promoter. (**A**) Heat maps show ChIP-qPCR for

p53, DREAM complex factors (E2F4, p130, KDM5a, B-MYB), co-activators (p300, CBP), PolII and the histone mark H3K27ac (associated with transcriptionally active chromatin), for ChIP lysates prepared 24 hours following addition of chemotherapeutics or nutlin-3A, as fold enrichment relative to the vehicle-treated controls. qPCR was performed using primers for the indicated gene promoters. A3B qPCR for the same ChIP DNAs are shown in Figure 4A. (**B**) Genome browser snapshots of the human chromosome 22 region within which the APOBEC3 genes are located, were generated using NF-κB p65 ChIP-seq data for HeLa and SW480 cells treated with TNFα for 1 and 16 hours, downloaded from NCBI GEO (GSE24518 and GSE102796). Also shown is p65 ChIP-seq data (GSE67295) for MCF7 cells treated with TNFα or IL1ß for 45mins. (**C, D**) Heat maps for ChIP-qPCR enrichment of NF-κB (RelA/p65, p50, RelB and p52) at p53-activated genes (p21, MDM2, A3C, A3H) and NF-κB target genes (ICAM1, IL8, CXCL1), using ChIP lysates prepared 24 hours following addition of chemotherapy agents, as fold enrichment relative to vehicle treatment. Accompanying Figure 4B and 4C, respectively. Note that the A3B results shown in this heat map are presented as bar charts in Figure 4B-C.

Supplementary Figure 4. NF-κB inhibitors prevent stimulation of APOBEC3B expression by chemotherapeutic drugs. (**A**) Heat map shows ChIP-qPCR for NF-κB (RelA/p65, p50, RelB and p52) subunits, using ChIP lysates prepared 24 hours following addition of chemotherapeutics ± NF-κB inhibitors BAY 11-7028 or TPCA1, as fold enrichment relative to vehicle controls. Accompanying the bar chart in Figure 4D, in which the same A3B ChIP-qPCR results are shown. (**B**) RNA prepared from T47D cells, 24 hours following drug addition, were used for RT-qPCR, normalised to GAPDH expression (n=3). Statistically significant reductions in gene expression for NF-κB inhibitor-treated samples, compared to the expression for each chemotherapy drug, are marked by asterisks ($p<0.05$). A3B expression using the same RNAs is shown in Figure 4E. (**C**) Total RNA was prepared from HCT116 cells treated as in (B). (**D**) T47D cells were transfected with siRNAs for the p50 or p65 NF-κB subunits, or with a control siRNA (siControl). The cells were treated with the indicated drugs 48 hours following transfection. RT-qPCR was performed using RNAs prepared after a further 24 hours (* = $p<0.05$ for n = 3).

Supplementary Figure 5. Chemotherapy induced A3B expression requires DNA-PKcs and ATM. (**A**) T47D cells were treated with an ATM inhibitor (KU55933) or with an ATR inhibitor (VE-821) for 24 hours. RT-qPCR shows that the ATM inhibitor does not alter A3B expression, while the ATR inhibitor reduced expression by approximately 25% (n=3; * = $p<0.05$). (**B**) RT-qPCR of HCT116 cells shows that the DNA-PKcs inhibitor NU7441 inhibits expression of A3B in a dose-dependent manner, without influencing expression of other APOBEC3 gene family members. KU55933 did not significantly affect A3B mRNA expression, whereas a 25% reduction in expression of all APOBEC3 genes was evident following treatment with VE-821) (* = $p<0.05$ for n = 3). (**C**) The ATM inhibitor KU55933 reduced etoposide and cisplatin stimulation of A3B expression in T47D cells. VE-821 treatment did not substantially reduce A3B expression (* = $p<0.05$ for n = 3), although a significant reduction in expression was noted for the etoposide treatment. (**D**) T47D cells were transfected with siRNAs for DNA-PKcs, ATM, ATR, or with a control siRNA (siControl). Drugs were added 48 hours following transfection and RNAs prepared after a further 24 hours (* = $p<0.05$ for n = 3). (**A-D**) All graphs show gene expression normalised to expression of GAPDH. (**E**) Protein lysates made 24 hours following drug addition were immunoblotted for the indicated protein. KU55933 was added to a final concentration of 5 µM. For parts (D) and (E) cisplatin and etoposide were added to a final concentration of 20µM and 10 µM, respectively.

Supplementary Figure 6. Chemical inhibition or siRNA-mediated DNA-PKcs knockdown inhibits chemotherapy-stimulated A3B expression. (**A-B**) NU7441 inhibits the chemotherapy drug stimulation of A3B expression in MDA-MB-453 (p53 mutant) and in ZR-75-1 (WT p53) cells (* = $p<0.05$ for n = 3). (**C**) Immunoblotting confirms inhibition of A3B expression by NU7441 in the presence or absence of cisplatin or etoposide. (**D-F**) Cisplatin and etoposide stimulation of A3B expression is similarly inhibited by NU7441 in cancer cell lines expressing WT or mutant p53 (* = $p<0.05$ for n = 3). (**G**) Cells were transfected with siRNAs for DNA-PKcs, or with a control siRNA (siControl). 48 hours following transfection the indicated drugs were added. RNAs were prepared for RT-qPCR after a further 24 hours (* = $p<0.05$ for n = 3).

Supplementary Figure 7. DNA-PKcs regulates ATM and AKT activities to regulate NF-κB activation of A3B expression. (**A, C**) Immunoblotting of T47D cell lysates following addition of cisplatin, etoposide ± 5 μM NU7441 or 5 μM MK2206 (AKT inhibitor). (**B**) Cells were treated with cisplatin or etoposide 48 hours following transfection with siDNA-PKcs, or siControl. Protein lysates were prepared after a further 24 hours.

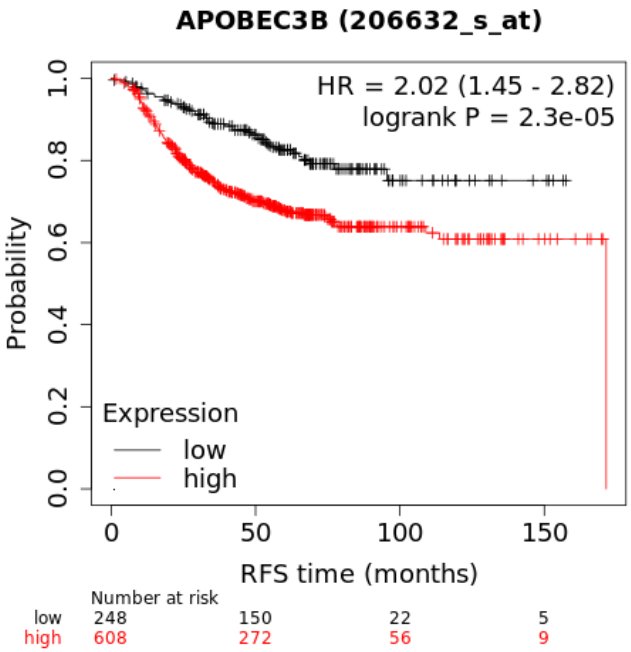
Supplementary Figure 8. Inhibition of DNA-PKcs reduces NF-κB recruitment to the A3B gene promoter in response to etoposide, cisplatin and hydroxyurea (HU). (A, C) The heat maps show ChIP-qPCR for NF-κB (RelA/p65, p50, RelB and p52) subunits, using ChIP lysates prepared 24 hours following addition of chemotherapeutics ± DNA-PKcs inhibitor NU7441, as fold enrichment relative to vehicle. (**B**) The T47D ChIP-qPCR results for the A3B gene shown in part (A) are also shown in the bar chart. Enrichment in shown relative to input.

Supplementary Figure 9. The DNA-PK/ATM/AKT/NF-kB pathway regulates APOBEC3B gene expression in transformed non-malignant and non-transformed non-malignant, breast epithelial cells. (**A, C**) MCF10A and PE003 cells, treated with drugs for 24 hours, were used for RNA extraction. Results for n=3 replicates are shown, asterisks denote treatment that show significant difference ($p<0.05$) from the vehicle control. (**B, D, E**) MCF10A, HMEC and PE003 cells were treated wth cisplatin and either vehicle or DNA-PK, ATM, AKT or NF-κB inhibitors. RNA was prepared after 24 hours. RT-qPCR was performed for n=3 replicates. Asterisks show treatments that are significantly different ($p<0.05$) from the cisplatin + DMSO-treated cells. (**F**) Protein lysates prepared from the transformed, non-malignant MCF10A breast cell line following addition of 20 μM cisplatin ± 5 μM NU7441 (NU), were used in the cytosine deaminase assay. Positions of the substrate and deamination product are shown. Deaminase product was quantified by densitometric analysis using Image J. The bar charts show the results for 3 independent experiments. Primary, untransformed, human mammary epithelial cells HMEC and PE003 cells, obtained from a breast cancer pleural effusion, were used in the deaminase assay, as above.

Supplementary Figure 10. Cisplatin-resistant ovarian cancer cells show increased sensitivity to inhibition of the DNA-PK/ATM/AKT/NF-κB pathway. (A-B) Cisplatin was used with PEA1 and PEA2 cells at concentrations ranging from 0.31 µM to 40 µM (2-fold serial dilutions), in the presence or absence of a DNA-PKcs inhibitor (NU7441), ATM inhibitor (KU55933), AKT inhibitor (MK2206) or the NF-κB inhibitor (TPCA1). All inhibitors were added to a final concentration of 1 µM. Growth was determined using the SRB assay after a further 96 hours. Cisplatin IC_{50} values, together with 95% confidence intervals, are shown for each combination treatment.

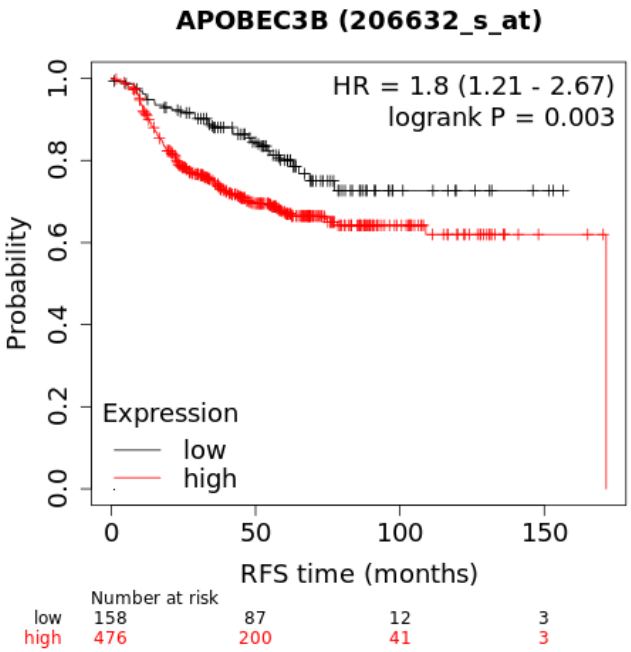
A

All chemotherapy treated patients

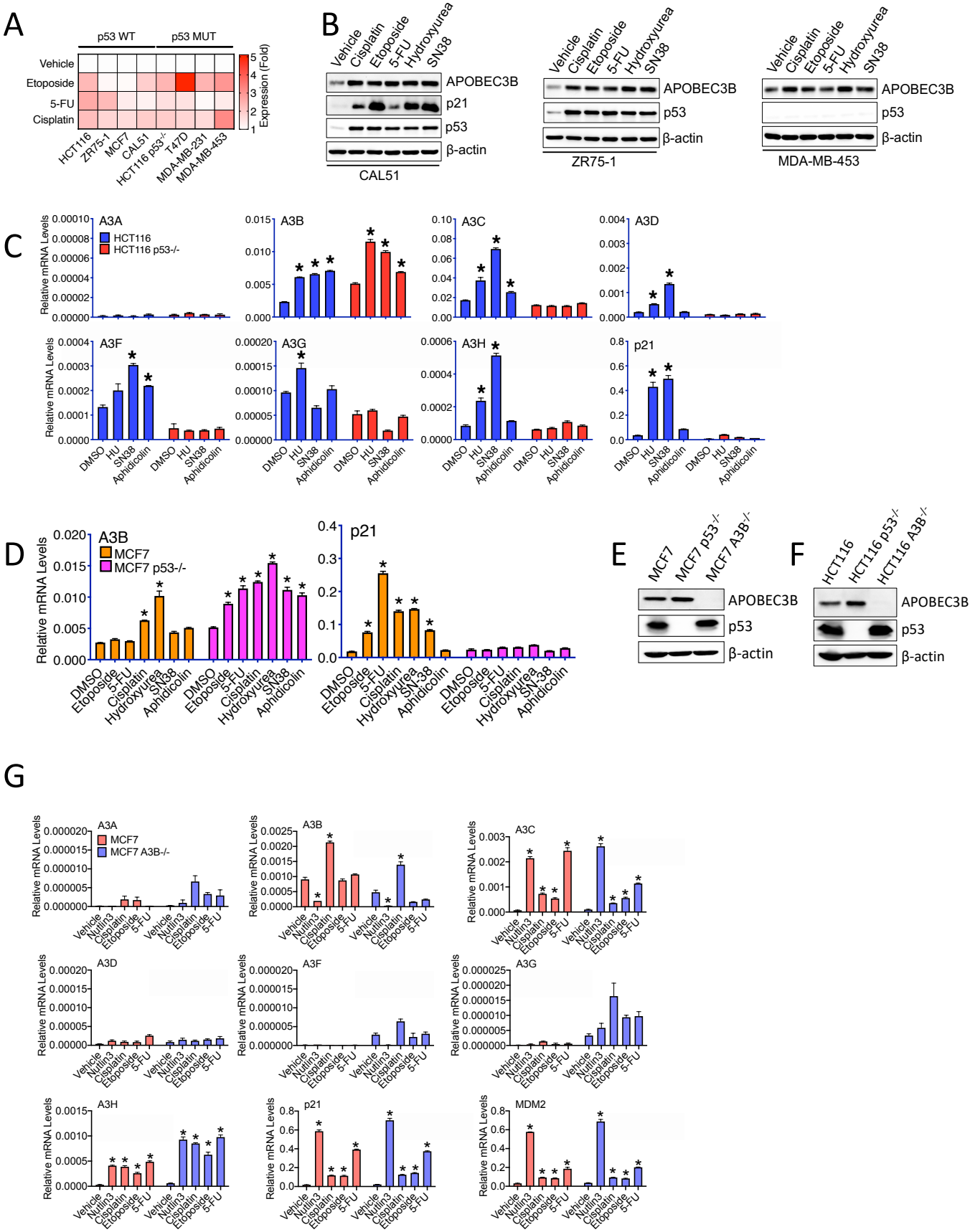


B

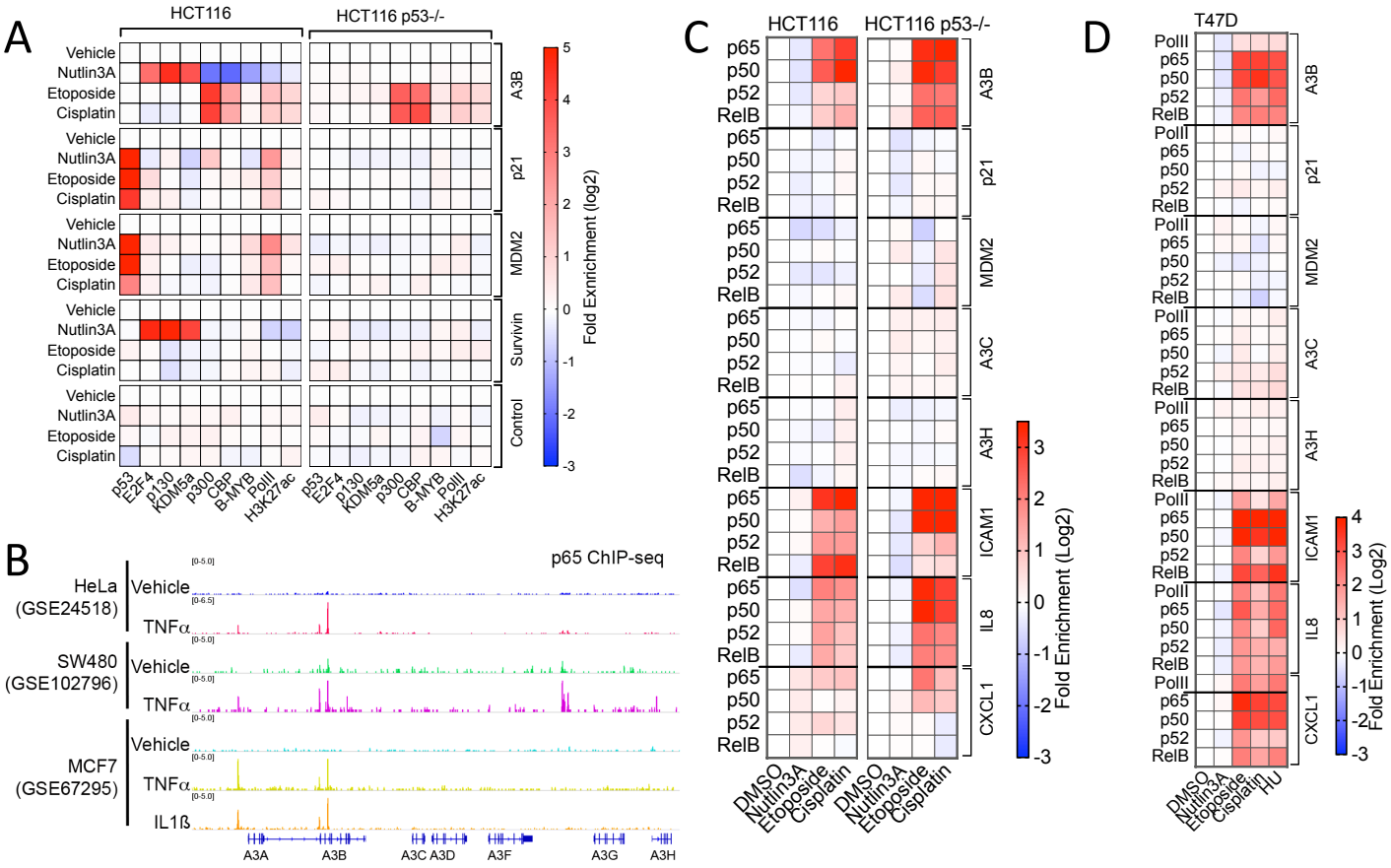
All chemotherapy treated patients Excluding those who received hormonal therapy



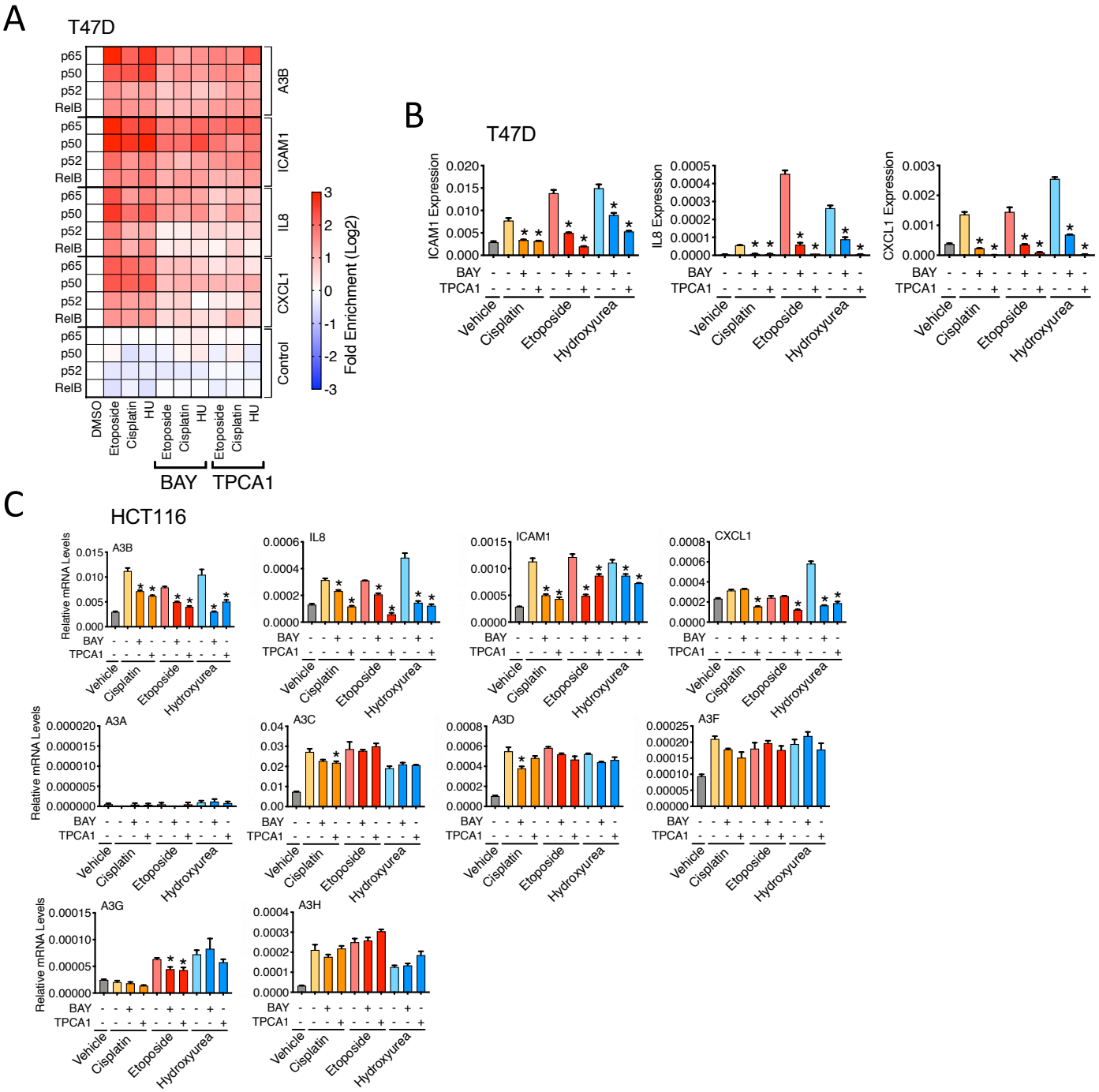
Supplementary Figure 1



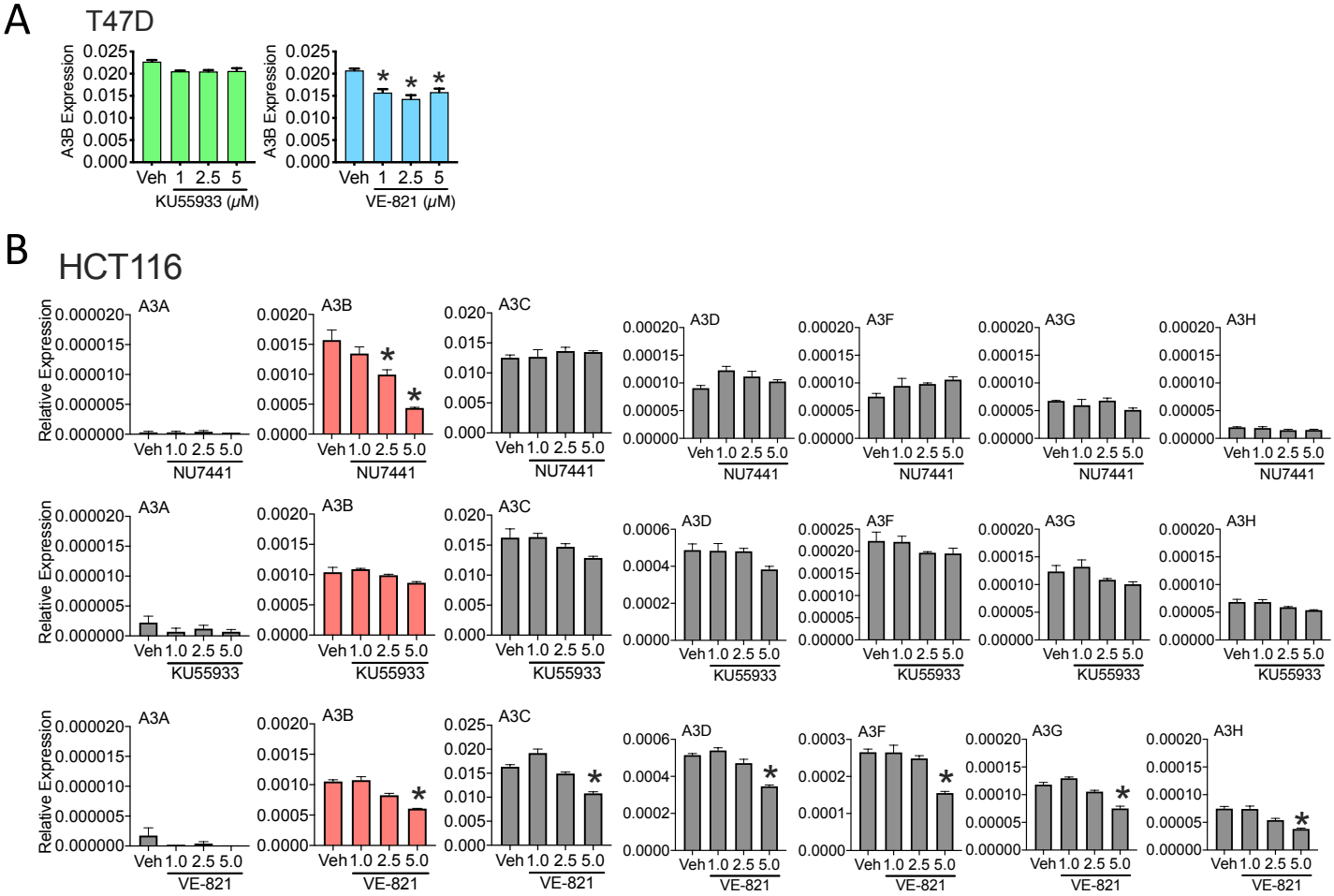
Supplementary Figure 2

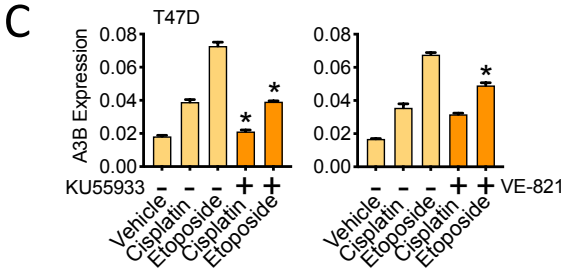


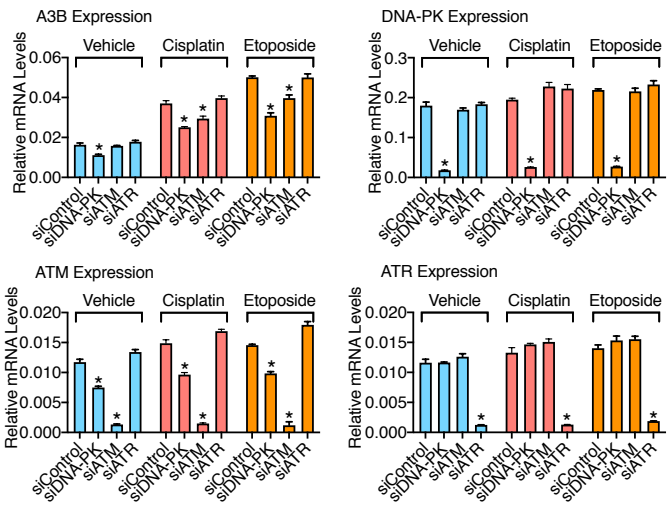
Supplementary Figure 3

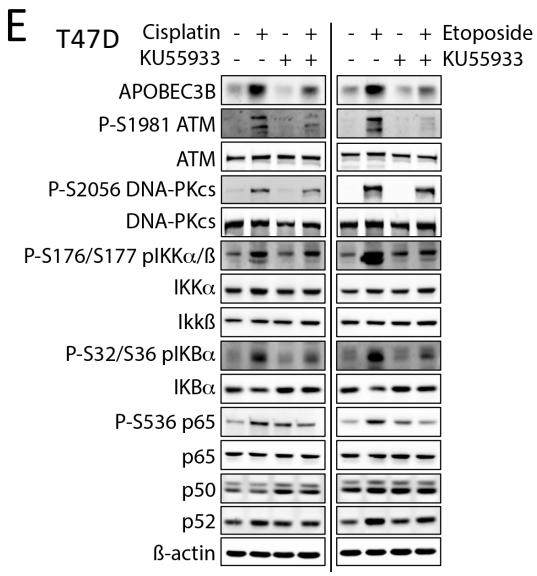


Supplementary Figure 4

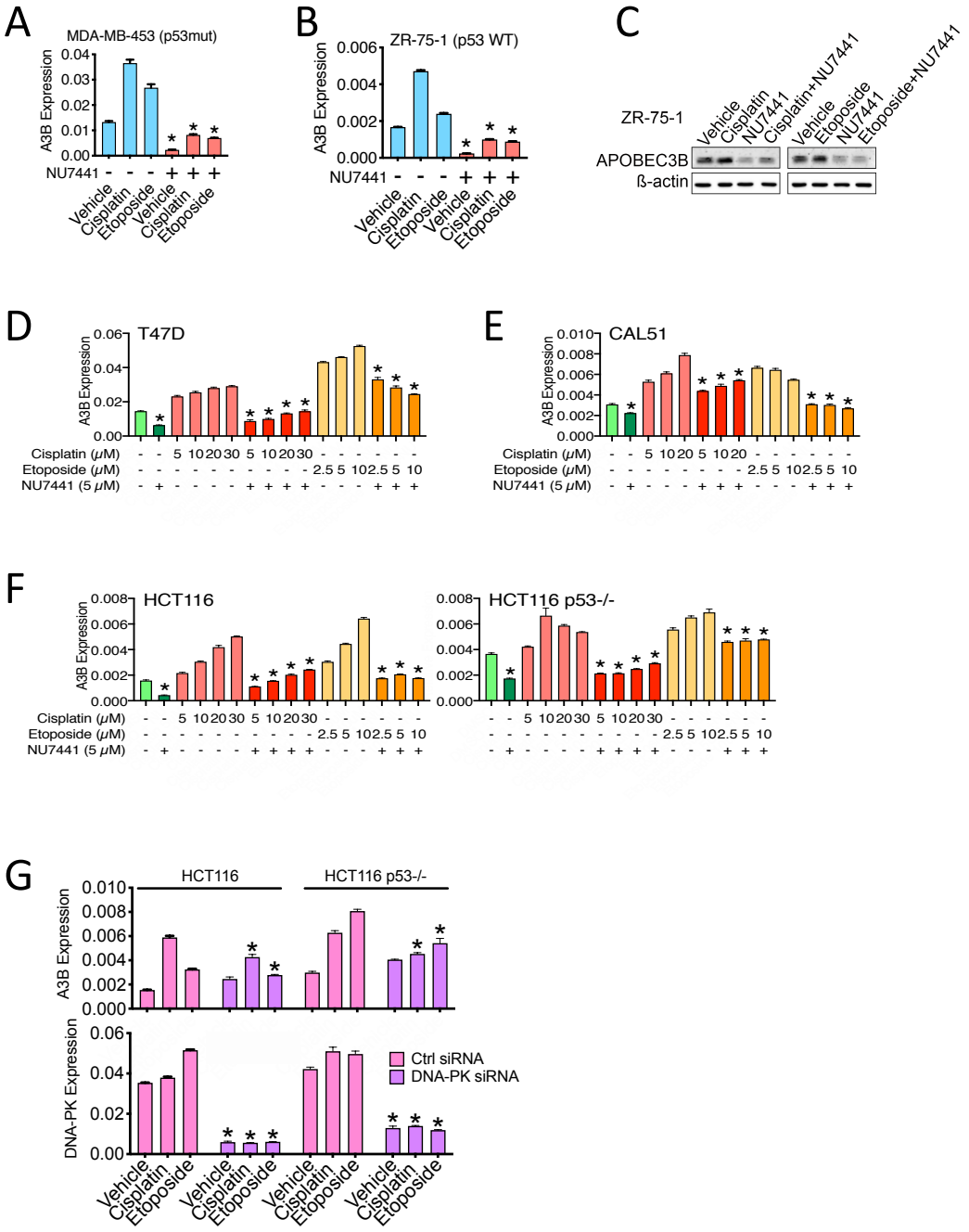




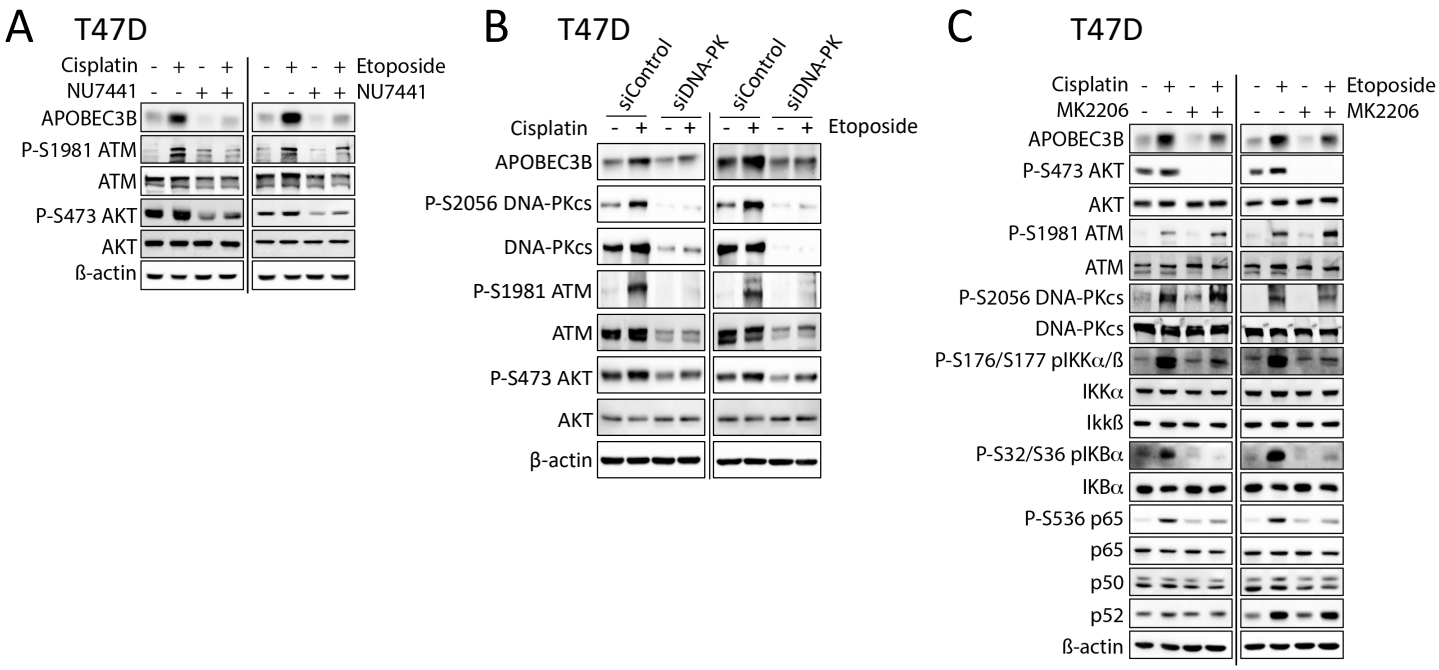




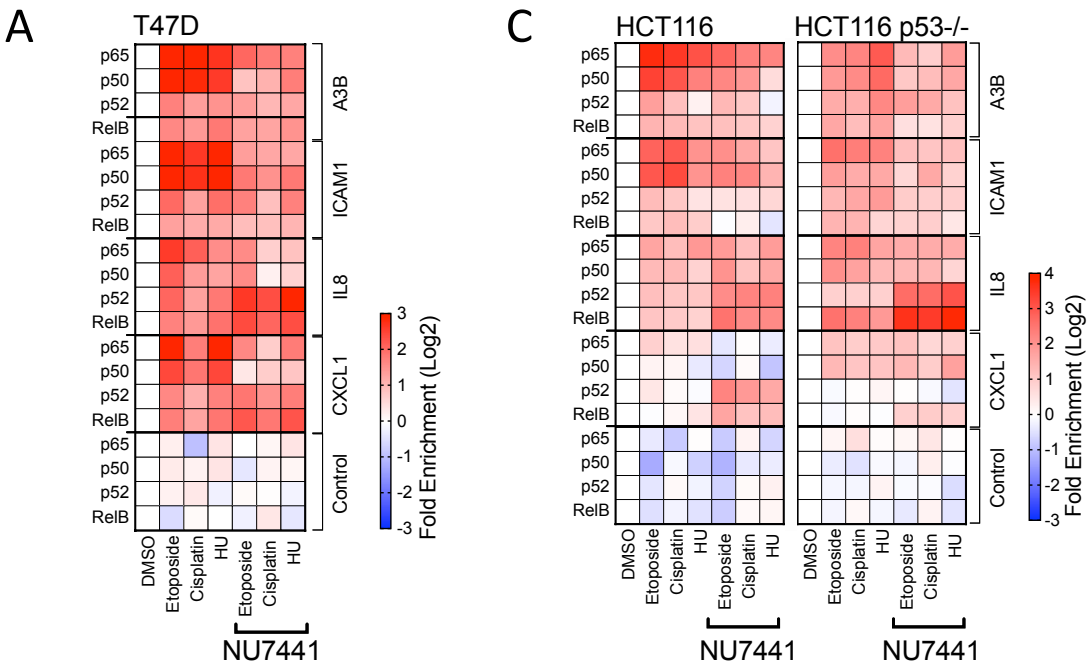
Supplementary Figure 5

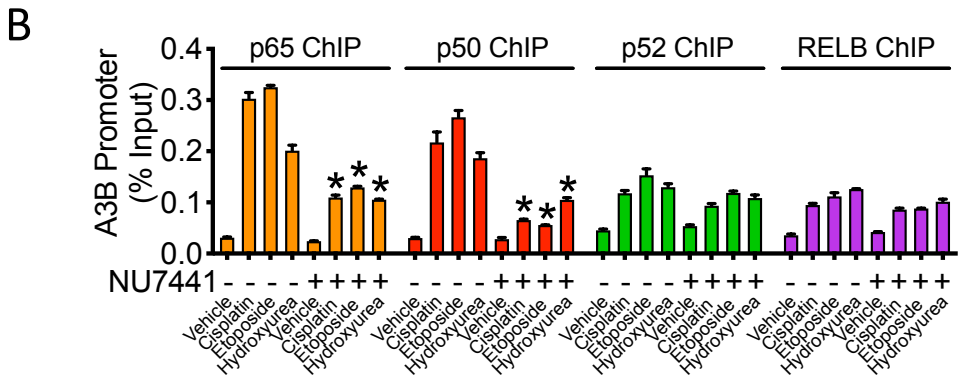


Supplementary Figure 6

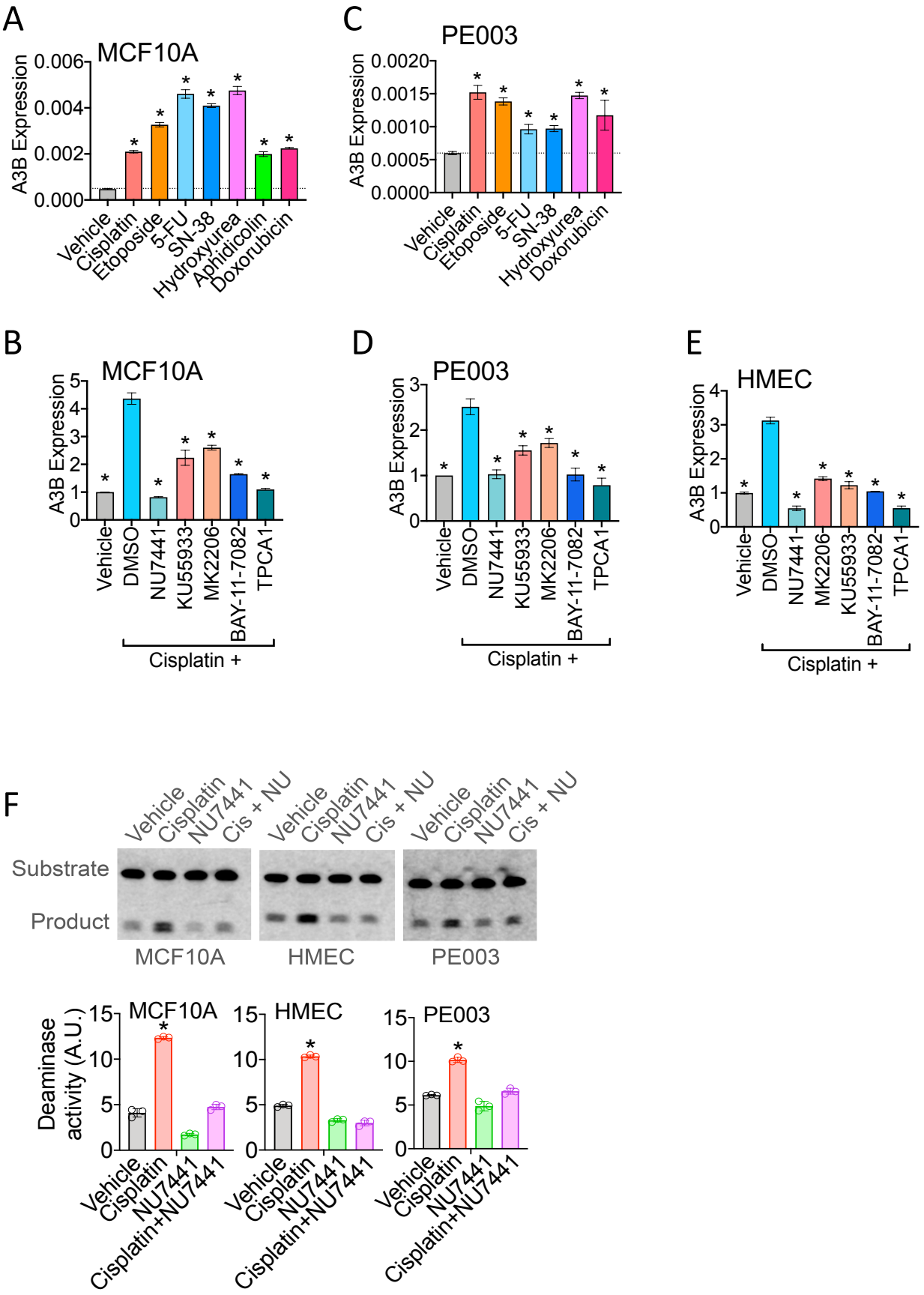


Supplementary Figure 7



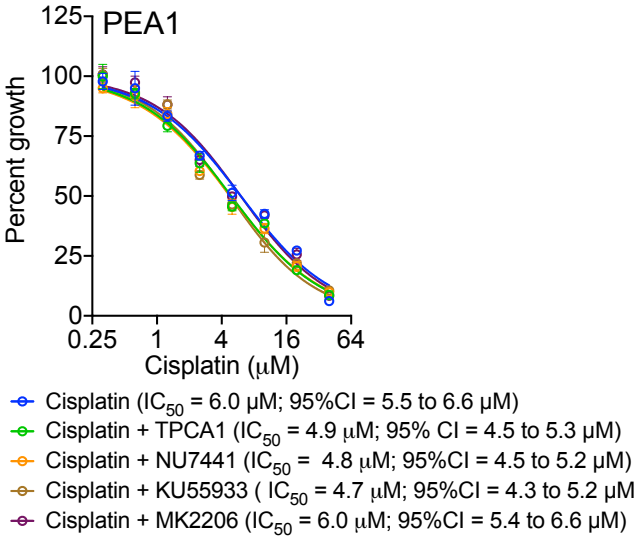


Supplementary Figure 8



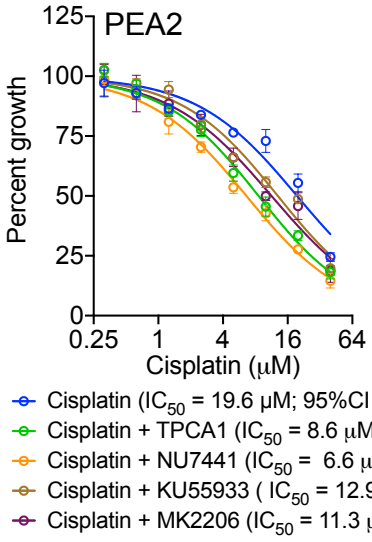
Supplementary Figure 9

A



Cisplatin (IC_{50} = 6.0 μM; 95%CI = 5.5 to 6.6 μM)
Cisplatin + TPCA1 (IC_{50} = 4.9 μM; 95% CI = 4.5 to 5.3 μM)
Cisplatin + NU7441 (IC_{50} = 4.8 μM; 95%CI = 4.5 to 5.2 μM)
Cisplatin + KU55933 (IC_{50} = 4.7 μM; 95%CI = 4.3 to 5.2 μM
Cisplatin + MK2206 (IC_{50} = 6.0 μM; 95%CI = 5.4 to 6.6 μM)

B



Cisplatin (IC_{50} = 19.6 μM; 95%CI = 17.1 to 22.6 μM)
Cisplatin + TPCA1 (IC_{50} = 8.6 μM; 95% CI = 8.0 to 9.2 μM)
Cisplatin + NU7441 (IC_{50} = 6.6 μM; 95%CI = 6.2 to 7.0 μM)
Cisplatin + KU55933 (IC_{50} = 12.9 μM; 95%CI = 11.6 to 14.5 μM
Cisplatin + MK2206 (IC_{50} = 11.3 μM; 95%CI = 10.1 to 12.7 μM)

Supplementary Figure 10